# Systematic construction of topological-nontopological hybrid universal quantum gates based on many-body Majorana fermion interactions

Motohiko Ezawa
*Department of Applied Physics, The University of Tokyo, 7-3-1 Hongo, Tokyo 113-8656, Japan*

(Received 17 August 2023; accepted 28 June 2024; published 9 July 2024)

Topological quantum computation by way of braiding of Majorana fermions is not universal quantum computation. There are several attempts to make universal quantum computation by introducing some additional quantum gates or quantum states. However, there is a serious problem in embedding an $M$-qubit quantum gate in the $N$-qubit system with $N > M$. This is an inherent problem to the Majorana system, where quantum gates for logical qubits become nonlocal in terms of physical qubits in general because braiding operations preserve the fermion parity. For instance, the CZ gate could not be embedded in the three-qubit system. We overcome this embedding problem by introducing $2(N+1)$-body interactions of Majorana fermions in the $N$-qubit system. A universal set of quantum gates is constructed for $N$ logical qubits, leading to topological-nontopological hybrid universal quantum computation. It would be more robust than conventional universal quantum computation because the quantum gates generated by braiding are topologically protected.

DOI: 10.1103/PhysRevB.110.045417

## I. INTRODUCTION

A quantum computer is a promising next-generation computer [1–3]. In order to execute any quantum algorithms, universal quantum computation is necessary [4–6]. There are various approaches to realize universal computation including superconductors [7], photonic systems [8], quantum dots [9], trapped ions [10], and nuclear magnetic resonance [11,12]. The Solovay-Kitaev theorem dictates that only the Hadamard gate, the T gate ($\pi/4$ phase-shift) gate, and the CNOT gate are enough for universal quantum computation. These one-qubit and two-qubit quantum gates can be embedded in larger qubits straightforwardly in these approaches.

Braiding of Majorana fermions is the most promising method for topological quantum computation [13–17]. There are various approaches to materialize Majorana fermions such as fractional quantum Hall effects [16,18–20], topological superconductors [21–27], and Kitaev spin liquids [28,29]. However, it can generate only a part of Clifford gate [30,31]. The entire Clifford gates are generated for two qubits but not for more than three qubits [31]. Furthermore, only the Clifford gates are not enough to exceed classical computers, which is known as the Gottesman-Knill theorem [32–34].

There is a proposal [13] that the two-body and four-body Majorana interaction operators are enough for universal quantum computation, where the four-body operation is given by $B_{1234}^{(4)} \equiv \exp[i(\pi/4)\gamma_4\gamma_3\gamma_2\gamma_1]$. In addition, there are several attempts to make universal quantum computation based on Majorana fermions [20,24,30,35–44] . It is claimed that the addition of the T gate or the magic state $|0\rangle + e^{i\pi/4}|1\rangle$ is enough for universal quantum computation because the elementary gates of the Solovay-Kitaev theorem are constructed. It is known as the magic state distillation. In these proposals it is taken for granted that an $M$-qubit quantum gate can be embedded in the $N$-qubit system when $N > M$. However, there are reports [45,46] to doubt it, where the CNOT gate and the CZ gate cannot be embedded in three logical qubits. Furthermore, it is impossible to construct the CCZ gate for three logical qubit systems. This problem has not so far been addressed seriously.

In this work, we investigate the origin of this embedding problem peculiar to the Majorana system. Because braiding preserves the fermion parity, it is necessary to construct logical qubits from physical qubits by taking a parity definite basis. We point out that a local quantum gate for logical qubits corresponds to a nonlocal quantum gate for physical qubits in general. Then it is highly nontrivial to embed an $M$-qubit quantum gate in the $N$-qubit system with $N > M$ in general. Even if the Hadamard gate, the T gate and the CNOT gate are constructed, it is not enough for universal quantum computation unless they can be embedded in the $N$-qubit system.

We overcome this embedding problem by introducing $2(N+1)$-body interactions of Majorana fermions in the $N$-qubit system preserving the fermion parity. Instead of embedding a certain gate in the $N+1$ physical system, we construct the concerned gate with the use of $2(N+1)$-body interactions from the beginning so as to respect the Solovay-Kitaev theorem. We systematically construct the Hadamard gate, the T gate, the CNOT gate, and then $C^s$ -phase shift gates, $C^s$NOT gates, $C^s$SWAP gates, and others with an arbitrary positive integer $s$. We have required the fermion parity preservation because it is beneficial to use the braiding process as much as possible due to its topological protection. By combining topological quantum gates generated by braiding and additional quantum gates generated by many-body interactions of Majorana fermions, topological-nontopological hybrid universal quantum computation is possible. It would be more robust than conventional universal quantum computation because the quantum gates generated by braiding are topologically protected.

 

## II. PHYSICAL QUBITS AND LOGICAL QUBITS

Majorana fermions are described by operators $\gamma_\alpha$ satisfying the anticommutation relations $\{\gamma_\alpha, \gamma_\beta\} = 2\delta_{\alpha\beta}$. The braid operator is defined by [14]

$$\mathcal{B}_{\alpha\beta} = \exp\left[\frac{\pi}{4}\gamma_\beta\gamma_\alpha\right] = \frac{1}{\sqrt{2}}(1 + \gamma_\beta\gamma_\alpha). \tag{1}$$

It satisfies $\mathcal{B}^4_{\alpha\beta} = 1$ and there is a corresponding antibraiding operator $\mathcal{B}^{-1}_{\alpha\beta} = \mathcal{B}^3_{\alpha\beta}$.

We adopt the dense encoding of Majorana fermions. The qubit basis is defined by [14]

$$|n_N n_{N-1} \cdots n_1 n_0\rangle_{\text{physical}} \equiv (c_0^\dagger)^{n_0}(c_1^\dagger)^{n_1}\cdots(c_{N-1}^\dagger)^{n_{N-1}}(c_N^\dagger)^{n_N}|0\rangle, \tag{2}$$

with $n_\alpha = 0$ or 1, where ordinary fermion operators are constructed from two Majorana fermions as

$$c_\alpha = (\gamma_{2\alpha+1} + i\gamma_{2\alpha+2})/2. \tag{3}$$

$2(N+1)$ Majorana fermions constitute $N+1$ physical qubits.

The braiding operation preserves the fermion parity,

$$P_{\alpha\beta} \equiv i\gamma_\beta\gamma_\alpha, \tag{4}$$

since it commutes with the braid operator $\mathcal{B}_{\alpha\beta}$, $[\mathcal{B}_{\alpha\beta}, P_{\alpha\beta}] = 0$. It means that if we start with the even-parity state $|00\cdots 0\rangle_{\text{physical}}$, then the states after any braiding process should have even fermion parity. Therefore, in order to construct $N$ logical qubits $|n_N \cdots n_2 n_1\rangle_{\text{logical}}$, $N+1$ physical qubits $|n_N \cdots n_2 n_1 n_0\rangle^{\text{even}}_{\text{physical}}$ are necessary [47–49], where $\sum_{\alpha=0}^{N} n_\alpha = 0 \mod 2$. We use the following abbreviation:

$$|\psi_N\rangle^{\text{even}}_{\text{phys}} \equiv |n_N \cdots n_2 n_1 n_0\rangle^{\text{even}}_{\text{physical}}, \tag{5}$$

$$|\psi_N\rangle_{\text{logi}} \equiv |n_N \cdots n_2 n_1\rangle_{\text{logical}}. \tag{6}$$

There are $(N+1)!$ correspondences between the logical and physical qubits in general. However, we adopt the following unique correspondence. When the logical qubit $|\psi_N\rangle_{\text{logi}}$ is given, we associate to it a physical qubit $|\psi_N\rangle^{\text{even}}_{\text{phys}}$ by adding one qubit $n_0$ uniquely so that $\sum_{\alpha=0}^{N} n_\alpha = 0 \mod 2$. On the other hand, when a physical qubit $|\psi_N\rangle^{\text{even}}_{\text{phys}}$ is given, we associate to it a logical qubit $|\psi_N\rangle_{\text{logi}}$ just by eliminating the qubit $n_0$ . An example reads as follows:

$$\begin{pmatrix} \overbrace{\qquad\qquad\qquad}^{N} \\ |0,\cdots,0,0,0\rangle \\ |0,\cdots,0,0,1\rangle \\ |0,\cdots,0,1,0\rangle \\ |0,\cdots,0,1,1\rangle \\ |0,\cdots,1,0,0\rangle \\ |0,\cdots,1,0,1\rangle \\ \cdots \end{pmatrix}_{\text{logical}} \Leftrightarrow \begin{pmatrix} \overbrace{\qquad\qquad\qquad}^{N+1} \\ |0,\cdots,0,0,0,0\rangle \\ |0,\cdots,0,0,1,1\rangle \\ |0,\cdots,0,1,0,1\rangle \\ |0,\cdots,0,1,1,0\rangle \\ |0,\cdots,1,0,0,1\rangle \\ |0,\cdots,1,0,1,0\rangle \\ \cdots \end{pmatrix}^{\text{even}}_{\text{physical}}. \tag{7}$$

We represent this correspondence as

$$|\psi_N\rangle_{\text{logi}} \Leftrightarrow |\psi_N\rangle^{\text{even}}_{\text{phys}}. \tag{8}$$

This correspondence is different from those in the previous works [13,45,46,48–50]. Accordingly, the detailed braiding process for quantum gates are slightly different from the previous ones [45,46,48–50].

A local quantum gate for logical qubits corresponds to a nonlocal quantum gate for physical qubits. For example, in order to flip the qubit state from 0 to 1 in the third qubit in logical qubits in Eq. (7), it is necessary to flip the first and fourth qubits simultaneously in physical qubits.

## III. EMBEDDING PROBLEM

There is a serious problem inherent to the Majorana system in embedding an $M$-qubit quantum gate in the $N$-qubit system with $N > M$. For example, the CZ gate is defined for the two-qubit system, which is trivially embed in the three-qubit system in usual quantum computation. However, this is not the case in quantum computation based on Majorana fermions. Indeed, it is impossible to realize the CZ gate only by braiding in the three-qubit system.

The embedding is defined as follows. Let us embed an $M$-qubit quantum gate in the $N$-qubit system with $M = N - 1$. The action of the braiding operator $\mathcal{B}_{\alpha\beta}$ on the $(N-1)$ logical qubits is represented by a quantum gate $U^{\text{even}}_{\alpha\beta}$ represented by a $2^{N-1} \times 2^{N-1}$ matrix $U^{\text{even}}_{\alpha\beta}$ as

$$\mathcal{B}_{\alpha\beta}|n_{N-1}\cdots n_1 n_0\rangle^{\text{even}}_{\text{phys}} = U^{\text{even}}_{\alpha\beta}|n_{N-1}\cdots n_1\rangle_{\text{logi}}. \tag{9}$$

If the action of the braiding operator $B_{\alpha\beta}$ on the $N$ logical qubits is represented by the quantum gate $I_2 \otimes U^{\text{even}}_{\alpha\beta}$ as

$$\mathcal{B}_{\alpha\beta}|n_N n_{N-1}\cdots n_1 n_0\rangle^{\text{even}}_{\text{phys}} = \left(I_2 \otimes U^{\text{even}}_{\alpha\beta}\right)|n_N n_{N-1}\cdots n_1\rangle_{\text{logi}}, \tag{10}$$

then the embedding is said to be possible.

We examine the condition (10). The additional qubit $n_N$ is either 0 or 1. When $n_N = 0$, Eq. (9) leads to

$$\mathcal{B}_{\alpha\beta}|0 n_{N-1}\cdots n_1 n_0\rangle^{\text{even}}_{\text{phys}} = |0\rangle \otimes U^{\text{even}}_{\alpha\beta}|n_{N-1}\cdots n_1\rangle_{\text{logi}}, \tag{11}$$

because $\sum_{\alpha=0}^{N-1} n_\alpha = 0 \mod 2$. However, when $n_N = 1$, because

$$|1 n_{N-1}\cdots n_1 n_0\rangle^{\text{even}}_{\text{phys}} = |1\rangle \otimes |n_{N-1}\cdots n_1 n_0\rangle^{\text{odd}}_{\text{phys}} \tag{12}$$

with $\sum_{\alpha=0}^{N-1} n_\alpha = 1 \mod 2$, we obtain

$$\mathcal{B}_{\alpha\beta}|1 n_{N-1}\cdots n_1 n_0\rangle^{\text{even}}_{\text{phys}} = |1\rangle \otimes U^{\text{odd}}_{\alpha\beta}|n_{N-1}\cdots n_1\rangle_{\text{logi}}, \tag{13}$$

where $U^{\text{odd}}_{\alpha\beta}$ is defined by the formula corresponding to Eq. (9) in the parity-odd sector. When $U^{\text{odd}}_{\alpha\beta} = U^{\text{even}}_{\alpha\beta}$, the embedding is possible because the condition (10) is satisfied with Eqs. (11) and (13). On the other hand, when $U^{\text{odd}}_{\alpha\beta} \neq U^{\text{even}}_{\alpha\beta}$, the embedding is impossible because the condition (10) is violated. We present an explicit example of the case where $U^{\text{odd}}_{\alpha\beta} \neq U^{\text{even}}_{\alpha\beta}$ in Appendix A 1: See (A11).

## IV. QUANTUM GATES

### A. 2*M*-body interactions

We overcome the embedding problem by introducing $2M$-body interactions to construct quantum gates acting on the $N$

logical qubits. We define the $2M$-body operator acting on $N+1$ physical qubits by

$$\mathcal{B}^{(2M)}_{\alpha_1\alpha_2\cdots\alpha_{2M}}(\theta) \equiv \exp\left[i^{(M-1)}\theta\gamma_{\alpha_{2M}}\cdots\gamma_{\alpha_2}\gamma_{\alpha_1}\right] = \cos\theta + i^{M-1}\gamma_{\alpha_{2M}}\cdots\gamma_{\alpha_2}\gamma_{\alpha_1}\sin\theta. \quad (14)$$

It keeps the parity, $[\mathcal{B}^{(2M)}_{\alpha_1\alpha_2\cdots\alpha_{2M-1}\alpha_{2M}}, P_{\alpha\beta}] = 0$, with the fermion parity operator (4), where $\gamma_\alpha$ and $\gamma_\beta$ are arbitrary Majorana operators. It satisfies the unitary condition,

$$\left(\mathcal{B}^{(2M)}_{\alpha_1\alpha_2\cdots\alpha_{2M-1}\alpha_{2M}}(\theta)\right)^\dagger \mathcal{B}^{(2M)}_{\alpha_1\alpha_2\cdots\alpha_{2M-1}\alpha_{2M}}(\theta) = I. \quad (15)$$

We introduce an abbreviation,

$$\mathcal{B}^{(2M)}_{\alpha}(\theta) \equiv \exp[i^{M-1}\theta\gamma_{\alpha+2M-1}\gamma_{\alpha+2M-2}\cdots\gamma_{\alpha+1}\gamma_\alpha]. \quad (16)$$

In what follows we adopt the convention that the direct product $U_N \otimes \cdots \otimes U_2 \otimes U_1$ of one-qubit gates $U_1$, $U_2$, …, and $U_N$ acts on the $N$ logical qubit state $|n_N\cdots n_2n_1\rangle_{\text{logi}}$, where $U_1$ acts on the first qubit $n_1$, $U_2$ acts on the second qubit $n_2$, and so on.

### B. Braid operator

The simplest one is the two-body operator $\mathcal{B}^{(2)}_{\alpha\beta}(\theta)$. It is the braiding operation with the choice of $\theta = \pi/4$,

$$\mathcal{B}_{\alpha\beta} = \mathcal{B}^{(2)}_{\alpha\beta}(\pi/4). \quad (17)$$

### C. Unitary gates

In the following, we study the action of the many-body interaction on a quantum gate for the $N$ logical qubit system,

$$\mathcal{B}^{(2M)}_{\alpha_1\alpha_2\cdots\alpha_{2M}}(\theta)|\psi_N\rangle^{\text{even}}_{\text{phys}} = U|\psi_N\rangle_{\text{logi}}, \quad (18)$$

which defines the quantum gate $U$ represented by a $2^N\times 2^N$ matrix.

### D. T gate

The T gate $U_T$ is given by setting $\theta = \pi/8$, which is an essential element of universal quantum computation. First, the local rotation along the $z$ axis is executed by the two-body interaction acting on the $N$-qubit system,

$$\mathcal{B}^{(2)}_{2n+1,2n+2}(\theta)|\psi_N\rangle^{\text{even}}_{\text{phys}} = I_{2^{N-n}} \otimes R_z(2\theta) \otimes I_{2^{n-1}}|\psi_N\rangle_{\text{logi}}, \quad (19)$$

where $R_z(\theta) = \exp[-i\theta\sigma_z/2]$ for $n \geqslant 2$. The T gate acting on the $n$ qubit in the $N$-qubit system is given by

$$U_T|\psi_N\rangle_{\text{logi}} = \mathcal{B}^{(2)}_{2n+1,2n+2}(\pi/8)|\psi_N\rangle^{\text{even}}_{\text{phys}}. \quad (20)$$

### E. Hadamard gate

We construct the Hadamard gate acting on the $n$th qubit of $N$ logical qubits as

$$U^{(n)}_H \equiv I_{2^{N-n}} \otimes U_H \otimes I_{2^{n-1}}, \quad (21)$$

where

$$U_H = R_z\left(\frac{\pi}{4}\right)R_x\left(\frac{\pi}{4}\right)R_z\left(\frac{\pi}{4}\right), \quad (22)$$

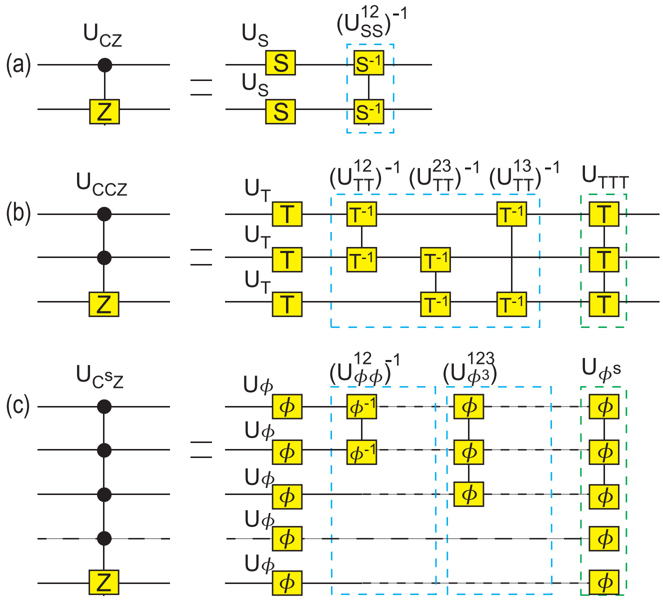


FIG. 1. (a) Decomposition of the CZ gate into a sequential application of the S gates and the inverse of the SS gate. (b) Decomposition of the CCZ gate into a sequential application of the T gates the TTT gate, and the inverse of the TT gates. (c) Decomposition of the $C^sZ$ gate into a sequential application of $\pi/2^{s+1}$ phase shift gate $U_\phi \equiv e^{-i\pi/2^{s+1}\sigma_z}$, $U_{\phi\phi} \equiv e^{-i\pi/2^{s+1}\sigma_z\otimes\sigma_z}$, $U_{\phi^3} \equiv e^{-i\pi/2^{s+1}\sigma_z\otimes\sigma_z\otimes\sigma_z}$, and $U_{\phi^s} \equiv e^{-i\pi/2^{s+1}\otimes_1^s\sigma_z}$.

with $R_x(\theta) = \exp[-i\theta\sigma_x/2]$ . The local rotation along the $x$ axis is executed by the $2n$-body interaction,

$$\mathcal{B}^{(2n)}_{2}(\theta)|\psi_N\rangle^{\text{even}}_{\text{phys}} = I_{2^{N-n}} \otimes R_x(2\theta) \otimes I_{2^{n-1}}|\psi_N\rangle_{\text{logi}}, \quad (23)$$

with the use of the abbreviation (16). Hence, the Hadamard gate acting on the $n$th qubit of $N$ logical qubits is

$$U^{(n)}_H|\psi_N\rangle_{\text{logi}} = \mathcal{B}^{(2n)}_2\left(\frac{\pi}{8}\right)\mathcal{B}_{2n+1,2n+2}\left(\frac{\pi}{8}\right)\mathcal{B}^{(2n)}_2\left(\frac{\pi}{8}\right)|\psi_N\rangle^{\text{even}}_{\text{phys}}, \quad (24)$$

by setting $2\theta = \pi/4$.

### F. CZ gates

The CZ gate for two-qubit systems is decomposed into the product of the ZZ rotation $R_{zz}$ and the Z rotation $R_z$ for the controlled and the target qubits,

$$U_{\text{CZ}} = e^{i\pi/4}U^{-1}_{\text{SS}}(U_{\text{S}} \otimes U_{\text{S}}), \quad (25)$$

where we have defined the S gate $U_{\text{S}} \equiv \exp[-i\pi\sigma_z/4]$ and the SS gate $U_{\text{SS}} \equiv \exp[-i\pi\sigma_z\otimes\sigma_z/4]$. See Fig. 1(a). The CZ gate $U^{m\to n}_{\text{CZ}}$ with the controlled qubit $m$ and the target qubit $n$ in $N$ qubits is given by

$$U^{m\to n}_{\text{CZ}}|\psi_N\rangle_{\text{logi}} = \mathcal{B}^{(4)}_{2m+1,2m+2,2n+1,2n+2}\left(-\frac{\pi}{4}\right) \times \mathcal{B}_{2m+1,2m+2}\left(\frac{\pi}{4}\right)\mathcal{B}_{2n+1,2n+2}\left(\frac{\pi}{4}\right)|\psi_N\rangle^{\text{even}}_{\text{phys}}. \quad (26)$$

See Eq. (B44) for the three-logical-qubit system and Eq. (B48) for the four-logical-qubit system in Appendix B5.

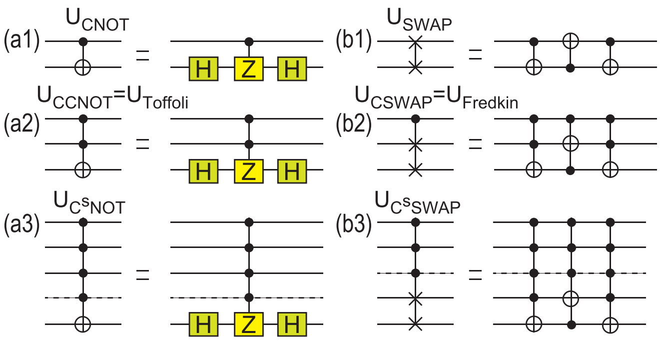


FIG. 2. (a1) Construction of the CNOT gate from the CZ gate and the Hadamard gates. (a2) Construction of the CCNOT (Toffoli) gate from the CCZ gate and the Hadamard gates. (a3) Construction of the C$^s$NOT gate from the C$^s$Z gate and the Hadamard gates. (b1) Construction of the SWAP gate from three CNOT gates. (b2) Construction of the CSWAP (Fredkin) gate from three Toffoli gates. (b3) Construction of the C$^s$SWAP gate from the C$^s$NOT gates.

### G. Universal quantum computation

According to the Solovay-Kitaev theorem, universal quantum computation is possible provided the Hadamard gate, the T gate, and the CNOT gate $U_{\text{CNOT}}$ are given. Instead of the CNOT gate we may use the CZ gate $U_{\text{CZ}}$ because of the relation

$$U_{\text{CNOT}} = (I_2 \otimes U_H)U_{\text{CZ}}(I_2 \otimes U_H), \tag{27}$$

where the Hadamard gate is applied to the second qubit. See Fig. 2(a1). By using Eq. (26), we obtain the CNOT gate $U_{\text{CNOT}}^{m\to n}$ with the controlled qubit $m$ and the target qubit $n$ embedded in $N$ qubits.

The SWAP gate is decomposed into a sequential application of three CNOT gates

$$U_{\text{SWAP}} = U_{\text{CNOT}}^{1\to 2}U_{\text{CNOT}}^{2\to 1}U_{\text{CNOT}}^{1\to 2}, \tag{28}$$

as shown in Fig. 2(b1).

The CCZ gate is decomposed into a sequential application of the T gates, the inverse of the TT gates and the TTT gate,

$$U_{\text{CCZ}} = e^{i\pi/8}U_{\text{TTT}}\big(U_{\text{TT}}^{13}\big)^{-1}\big(U_{\text{TT}}^{23}\big)^{-1}\big(U_{\text{TT}}^{12}\big)^{-1}(U_T \otimes U_T \otimes U_T), \tag{29}$$

where we have defined the T gate $U_T$, the TT gate $U_{\text{TT}}$, and the TTT gate $U_{\text{TTT}}$,

$$U_T = \exp\left[-i\pi\sigma_z/8\right], \quad U_{\text{TT}} = \exp\left[-i\pi\sigma_z \otimes \sigma_z/8\right],$$
$$U_{\text{TTT}} = \exp\left[-i\pi\sigma_z \otimes \sigma_z \otimes \sigma_z/8\right], \tag{30}$$

as shown in Fig. 1(b).

The Toffoli (CCNOT) gate is constructed by applying the Hadamard gate to the CCZ gate as in

$$U_{\text{Toffloi}} = (I_4 \otimes U_H)U_{\text{CCZ}}(I_4 \otimes U_H). \tag{31}$$

See Fig. 2(a2). The Fredkin (CSWAP) gate is constructed by a sequential application of three Toffoli gates as in

$$U_{\text{Fredkin}} = U_{\text{Toffoli}}^{(3,2)\to 1}U_{\text{Toffoli}}^{(3,1)\to 2}U_{\text{Toffoli}}^{(3,2)\to 1}, \tag{32}$$

where $U_{\text{Toffoli}}^{(p,q)\to r}$ indicates that the controlled qubits are $p$ and $q$ while the target qubit is $r$. See Fig. 2(b2).

Similarly, we systematically construct the C$^s$-phase shift gate as shown in Fig. 1(c). Details are shown in Eq. (C7) in Appendix C.

The C$^s$NOT gate is constructed from C$^s$Z gate as

$$U_{\text{C}^s\text{NOT}} = \big(I_{2s-2} \otimes U_H^{(s)}\big)U_{\text{C}^s\text{Z}}\big(I_{2s-2} \otimes U_H^{(s)}\big), \tag{33}$$

where the Hadamard gate is applied to $n$th qubit. See Fig. 2(a3).

The C$^s$SWAP gate is constructed from the C$^s$Z gate as

$$U_{\text{C}^s\text{SWAP}} = U_{\text{C}^s\text{NOT}}^{\overline{1}\to 1}U_{\text{C}^s\text{NOT}}^{\overline{2}\to 2}U_{\text{C}^s\text{NOT}}^{\overline{1}\to 1}, \tag{34}$$

where $U_{\text{C}^s\text{NOT}}^{\overline{p}\to p}$ indicates that the target qubit is $p$ and the others are controlled qubits, where $\overline{p}$ indicates the complementary qubits of the qubit $p$. See Fig. 2(b3).

Appendixes B and C are prepared for detailed analysis in the case of small qubits to make clear a general analysis for the $N$-qubit system.

## V. EXPERIMENTAL REALIZATION

The two-body operation is realized by the unitary dynamics during $0 \leqslant t \leqslant T$,

$$\mathcal{B}_{\alpha\beta}(\theta) = \exp[\theta\gamma_\beta\gamma_\alpha] = \exp\left[iHt/\hbar\right], \tag{35}$$

with $H = (\hbar\theta/iT)\gamma_\beta\gamma_\alpha$. A $2N$-body Majorana operation is realized by a dynamics driven by $2N$-body interaction of Majorana fermions during $0 \leqslant t \leqslant T$,

$$\mathcal{B}_{\alpha}^{(2N)}(\theta) = \exp\left[iHt/\hbar\right], \tag{36}$$

with $H = (i^{N-2}\hbar\theta/T)\gamma_{2N}\gamma_{2N-1}\cdots\gamma_2\gamma_1$.

There are two possible experimental realizations. One is based on topological superconductors. $2N$-body interaction is represented in terms of the $N$-body density operator [51],

$$\gamma_{2\alpha_1-1}\gamma_{2\alpha_1}\gamma_{2\alpha_2-1}\gamma_{2\alpha_2}\cdots\gamma_{2\alpha_N-1}\gamma_{2\alpha_N}$$
$$= i^N\big(2\rho_{\alpha_1}-1\big)\big(2\rho_{\alpha_2}-1\big)\cdots\big(2\rho_{\alpha_N}-1\big), \tag{37}$$

by using the realization $i\gamma_{2\alpha-1}\gamma_{2\alpha} = 2\rho_\alpha - 1$, where $\rho_\alpha = c_\alpha^\dagger c_\alpha$. The other is the Kitaev spin liquid system. $2N$-body Majorana interactions are written in the form [75,77]

$$\gamma_{\alpha_1}^A\gamma_{\alpha_1}^B\gamma_{\alpha_2}^A\gamma_{\alpha_2}^B\cdots\gamma_{\alpha_N}^A\gamma_{\alpha_N}^B \propto \sigma_{\alpha_1}^z\sigma_{\alpha_2}^z\cdots\sigma_{\alpha_N}^z. \tag{38}$$

See Appendix D for details.

## VI. DISCUSSIONS

We have analyzed the embedding problem inherent to the Majorana system and shown that universal quantum computation is possible by introducing many-body interactions of Majorana fermions. The proposed quantum gates based on many-body interactions of Majorana fermions are not topologically protected. It is an interesting problem to construct quantum algorithm, where the number of topologically protected quantum gates are maximized and the decoherence problem is minimized.

We have adopted the dense encoding described by Eq. (7), where $2(N+1)$ Majorana fermions are used for $N$ qubits. On the other hand, $4N$ Majorana fermions are used for $N$ qubits in the sparce encoding [24,78]. The embedding problem also exists in the sparce encoding, which is solved by introducing many-body Majorana interactions as in the case of the dense encoding. The dense encoding is more efficient than the sparce encoding because the number of the necessary gates is smaller. See details in Appendix E.

In passing we note that quantum simulation on Majorana fermions is studied in superconducting qubits [52–54]. In addition, the Kitaev chain is realized in coupled quantum dots [55].


## ACKNOWLEDGMENTS

This work is supported by CREST, JST (Grant No. JPMJCR20T2) and Grants-in-Aid for Scientific Research from MEXT KAKENHI (Grant No. 23H00171).


## APPENDIX A: RESULTS ON CONVENTIONAL BRAIDING

### 1. Embedding

We consider a one-dimensional chain of Majorana fermions and only consider the braiding between adjacent Majorana fermions. We denote $\mathcal{B}_\alpha \equiv \mathcal{B}_{\alpha,\alpha+1}$. The braid operators $\mathcal{B}_\alpha$ satisfies the Artin braid group relation [56]

$$\mathcal{B}_\alpha \mathcal{B}_\beta = \mathcal{B}_\beta \mathcal{B}_\alpha \quad \text{for} \quad |\alpha - \beta| \geqslant 2,$$
$$\mathcal{B}_\alpha \mathcal{B}_{\alpha+1} \mathcal{B}_\alpha = \mathcal{B}_{\alpha+1} \mathcal{B}_\alpha \mathcal{B}_{\alpha+1}. \tag{A1}$$

The embedding of an $M$-qubit quantum gate to an $N$-qubit system with $M < N$ is a nontrivial problem in braiding of Majorana fermions. There are two partial solutions. One is setting additional qubits to be 0 as ancilla qubits, where every quantum gates can be embedded. The other is not to use the braiding $\mathcal{B}_1$. We discuss both of these in what follows.

### 2. One logical qubit

We discuss how to construct the one logical qubit [14]. Two ordinary fermions $c_1$ and $c_2$ are introduced from four Majorana fermions as

$$c_1 = \tfrac{1}{2}(\gamma_1 + i\gamma_2), \quad c_2 = \tfrac{1}{2}(\gamma_3 + i\gamma_4). \tag{A2}$$

The basis of physical qubits is given by

$$\begin{aligned} &|\psi_1\rangle_{\text{physical}} \\ &\quad = (|0\rangle, c_1^\dagger|0\rangle, c_2^\dagger|0\rangle, c_1^\dagger c_2^\dagger|0\rangle)^t \\ &\quad \equiv (|0,0\rangle_{\text{physical}}, |0,1\rangle_{\text{physical}}, |1,0\rangle_{\text{physical}}, |1,1\rangle_{\text{physical}})^t. \end{aligned} \tag{A3}$$

By taking the even-parity basis as

$$|\psi_1\rangle_{\text{logical}} = \begin{pmatrix} |0\rangle \\ |1\rangle \end{pmatrix}_{\text{logical}} \Leftrightarrow \begin{pmatrix} |0,0\rangle \\ |1,1\rangle \end{pmatrix}_{\text{physical}} \equiv |\psi_1\rangle_{\text{physical}}^{\text{even}}, \tag{A4}$$

the one logical qubit is constructed by projecting the two physical qubits. This is the simplest example of Eq. (7) in the main text.

#### Quantum gates

The braid operator $\mathcal{B}_1$ is written in terms of fermion operators,

$$\mathcal{B}_1 = \frac{1}{\sqrt{2}}(1 + \gamma_2\gamma_1) = \frac{1}{\sqrt{2}}(1 + ic_1^\dagger c_1 - ic_1 c_1^\dagger), \tag{A5}$$

which operates on the two physical qubits (A3) as [14]

$$\begin{aligned} \mathcal{B}_1|\psi_1\rangle_{\text{physical}} &= e^{-i\pi/4}\begin{pmatrix} 1 & 0 & 0 & 0 \\ 0 & i & 0 & 0 \\ 0 & 0 & 1 & 0 \\ 0 & 0 & 0 & i \end{pmatrix}\begin{pmatrix} |0,0\rangle \\ |0,1\rangle \\ |1,0\rangle \\ |1,1\rangle \end{pmatrix}_{\text{physical}} \\ &\equiv U_1 \begin{pmatrix} |0,0\rangle \\ |0,1\rangle \\ |1,0\rangle \\ |1,1\rangle \end{pmatrix}_{\text{physical}}. \end{aligned} \tag{A6}$$

Taking the even-parity basis, the action is

$$\begin{aligned} \mathcal{B}_1|\psi_1\rangle_{\text{physical}}^{\text{even}} &= e^{-i\pi/4}\begin{pmatrix} 1 & 0 \\ 0 & i \end{pmatrix}\begin{pmatrix} |0\rangle \\ |1\rangle \end{pmatrix}_{\text{logical}} \\ &\equiv U_1^{\text{even}}\begin{pmatrix} |0\rangle \\ |1\rangle \end{pmatrix}_{\text{logical}}. \end{aligned} \tag{A7}$$

The braid operator $\mathcal{B}_1$ is represented by

$$U_1^{\text{even}} = e^{-i\pi/4}U_{\text{S}}, \tag{A8}$$

in terms of the S gate defined by

$$U_{\text{S}} \equiv \text{diag}(1, i), \tag{A9}$$

when it acts on the one logical qubit.

On the other hand, taking the odd-parity basis in Eq. (A6), the action is

$$\begin{aligned} \mathcal{B}_1|\psi_1\rangle_{\text{physical}}^{\text{even}} &= e^{-i\pi/4}\begin{pmatrix} i & 0 \\ 0 & 1 \end{pmatrix}\begin{pmatrix} |0\rangle \\ |1\rangle \end{pmatrix}_{\text{logical}} \\ &\equiv U_1^{\text{odd}}\begin{pmatrix} |0\rangle \\ |1\rangle \end{pmatrix}_{\text{logical}}. \end{aligned} \tag{A10}$$

It follows from Eq. (A7) and Eq. (A10) that

$$U_1^{\text{even}} \neq U_1^{\text{odd}}. \tag{A11}$$

This is the simplest example of the embedding problem in the main text. In the following, we only consider the even parity.

In what follows we represent Eq. (A7) or generalized ones by

$$\mathcal{B}_1 \simeq U_1 \tag{A12}$$

or generalized ones, where $\mathcal{B}_1$ acts on even-parity physical qubits which is represented by a matrix $U_1$ acting on logical qubits.

The braid operator $\mathcal{B}_2$ is written in terms of fermion operators,

$$\begin{aligned} \mathcal{B}_2 &= \frac{1}{\sqrt{2}}(1 + \gamma_3\gamma_2) \\ &= \frac{1}{\sqrt{2}}(1 + ic_2 c_1^\dagger + ic_2^\dagger c_1^\dagger - ic_2 c_1 - ic_2^\dagger c_1). \end{aligned} \tag{A13}$$

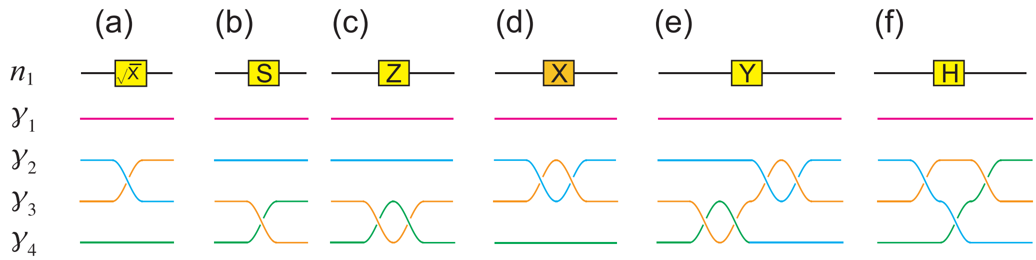


FIG. 3. (a) Square-root of NOT gate, (b) S gate, (c) Pauli Z gate, (d) Pauli X gate, (e) Pauli Y gate, and (f) Hadamard gate.

It operates on the two physical qubits as [14]

$$\mathcal{B}_2|\psi_1\rangle_{\text{physical}} = \frac{1}{\sqrt{2}}\begin{pmatrix} 1 & 0 & 0 & -i \\ 0 & 1 & -i & 0 \\ 0 & -i & 1 & 0 \\ -i & 0 & 0 & 1 \end{pmatrix}\begin{pmatrix} |0,0\rangle \\ |0,1\rangle \\ |1,0\rangle \\ |1,1\rangle \end{pmatrix}_{\text{physical}} = U_{xx}\begin{pmatrix} |0,0\rangle \\ |0,1\rangle \\ |1,0\rangle \\ |1,1\rangle \end{pmatrix}_{\text{physical}}, \tag{A14}$$

where

$$U_{xx} \equiv \frac{1}{\sqrt{2}}\begin{pmatrix} 1 & 0 & 0 & -i \\ 0 & 1 & -i & 0 \\ 0 & -i & 1 & 0 \\ -i & 0 & 0 & 1 \end{pmatrix} = \exp\left[-i\frac{\pi}{4}\sigma_x \otimes \sigma_x\right]. \tag{A15}$$

In the even-parity basis, the action is

$$\mathcal{B}_2|\psi_1\rangle^{\text{even}}_{\text{physical}} = \frac{1}{\sqrt{2}}\begin{pmatrix} 1 & -i \\ -i & 1 \end{pmatrix}|\psi_1\rangle_{\text{logical}} = \exp\left[-i\frac{\pi}{4}\sigma_x\right]|\psi_1\rangle_{\text{logical}} \equiv R_x|\psi_1\rangle_{\text{logical}}. \tag{A16}$$

It is represented as

$$\mathcal{B}_2 \simeq \frac{1}{\sqrt{2}}\begin{pmatrix} 1 & -i \\ -i & 1 \end{pmatrix} = e^{-i\pi/4}U_{\sqrt{X}}, \tag{A17}$$

where $U_{\sqrt{X}}$ is the square root of X gate defined by

$$U_{\sqrt{X}} \equiv \frac{1}{2}\begin{pmatrix} 1+i & 1-i \\ 1-i & 1+i \end{pmatrix}. \tag{A18}$$

The corresponding braiding is shown in Fig. 3(a).

The braiding operator $\mathcal{B}_3$ is written in terms of fermion operators,

$$\mathcal{B}_3 = \frac{1}{\sqrt{2}}(1+\gamma_4\gamma_3) = \frac{1}{\sqrt{2}}(1+ic_2^\dagger c_2 - ic_2c_2^\dagger), \tag{A19}$$

which operates on two physical qubits (A3) as [14]

$$\mathcal{B}_3|\psi_1\rangle_{\text{physical}} = e^{-i\pi/4}\begin{pmatrix} 1 & 0 & 0 & 0 \\ 0 & 1 & 0 & 0 \\ 0 & 0 & i & 0 \\ 0 & 0 & 0 & i \end{pmatrix}\begin{pmatrix} |0,0\rangle \\ |0,1\rangle \\ |1,0\rangle \\ |1,1\rangle \end{pmatrix}_{\text{physical}}. \tag{A20}$$

In the even-parity basis, the action is the same as (A8),

$$\mathcal{B}_3 \simeq e^{-i\pi/4}U_S, \tag{A21}$$

where the S gate is defined by (A9). The corresponding braiding is shown in Fig. 3(b).

The Pauli Z gate $U_Z$ is given by double braiding of $\mathcal{B}_3$,

$$U_Z \equiv \text{diag}(1,-1) = U_S^2 \simeq i\mathcal{B}_3^2. \tag{A22}$$

The corresponding braiding is shown in Fig. 3(c).

The Pauli X gate (NOT gate) is given [16] by double braiding of $\mathcal{B}_2$,

$$U_X \equiv \begin{pmatrix} 0 & 1 \\ 1 & 0 \end{pmatrix} \simeq i\mathcal{B}_2^2. \tag{A23}$$

The corresponding braiding is shown in Fig. 3(d).

Then, the Pauli Y gate is given by sequential applications of $\mathcal{B}_2$ and $\mathcal{B}_3$,

$$U_Y \equiv \begin{pmatrix} 0 & -i \\ i & 0 \end{pmatrix} = iU_XU_Z \simeq -\mathcal{B}_2^2\mathcal{B}_3^2. \tag{A24}$$

The corresponding braiding is shown in Fig. 3(e).

The Hadamard gate is defined by

$$U_H \equiv \frac{1}{\sqrt{2}}\begin{pmatrix} 1 & 1 \\ 1 & -1 \end{pmatrix}. \tag{A25}$$

It is known to be generated by triple braids as [45,50]

$$U_H \simeq i\mathcal{B}_2\mathcal{B}_3\mathcal{B}_2. \tag{A26}$$

The corresponding braiding is shown in Fig. 3(f).

### 3. Two logical qubits

In order to construct two logical qubits, we use six Majorana fermions $\gamma_1$, $\gamma_2$, $\gamma_3$, $\gamma_4$, $\gamma_5$, and $\gamma_6$. Three ordinary fermion operators are given by

$$c_1 = \tfrac{1}{2}(\gamma_1 + i\gamma_2), \quad c_2 = \tfrac{1}{2}(\gamma_3 + i\gamma_4), \quad c_3 = \tfrac{1}{2}(\gamma_5 + i\gamma_6). \tag{A27}$$

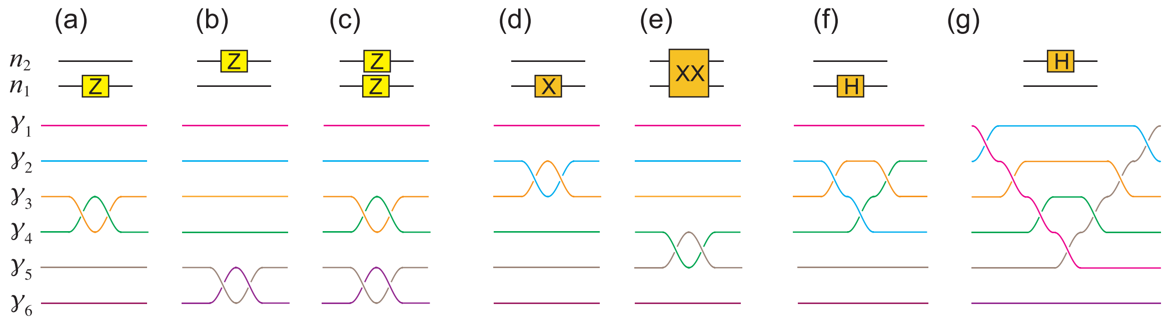


FIG. 4. The braiding process for Pauli gates. (a) Pauli Z gate embedded in the first qubit, (b) Pauli Z gate embedded in the second qubit, (c) two Pauli Z gates are embedded in the first and the second qubits, (d) Pauli X gate embedded in the first qubit, (e) Two Pauli X gates are embedded in the first and the second qubits, (f) Hadamard gate embedded in the first qubit, and (g) Hadamard gate embedded in the second qubit.

The basis of physical qubits are given by

$$\Psi_{\text{physical}} = (|0\rangle, c_1^\dagger|0\rangle, c_2^\dagger|0\rangle, c_1^\dagger c_2^\dagger|0\rangle, c_3^\dagger|0\rangle, c_1^\dagger c_3^\dagger|0\rangle, c_2^\dagger c_3^\dagger|0\rangle, c_1^\dagger c_2^\dagger c_3^\dagger|0\rangle)^t$$
$$\equiv (|0,0,0\rangle_{\text{physical}}, |0,0,1\rangle_{\text{physical}}, |0,1,0\rangle_{\text{physical}}, |0,1,1\rangle_{\text{physical}}, |1,0,0\rangle_{\text{physical}}, |1,0,1\rangle_{\text{physical}}, |1,1,0\rangle_{\text{physical}}, |1,1,1\rangle_{\text{physical}})^t. \quad \text{(A28)}$$

The explicit braid operators on the physical qubits are

$$\begin{aligned}\mathcal{B}_1 &= I_2 \otimes I_2 \otimes U_S,\\ \mathcal{B}_2 &= I_2 \otimes U_{xx},\\ \mathcal{B}_3 &= I_2 \otimes U_S \otimes I_2,\\ \mathcal{B}_4 &= U_{xx} \otimes I_2,\\ \mathcal{B}_5 &= U_S \otimes I_2 \otimes I_2.\end{aligned} \quad \text{(A29)}$$

Two logical qubits are constructed from three physical qubits as

$$\begin{pmatrix}|0,0\rangle\\|0,1\rangle\\|1,0\rangle\\|1,1\rangle\end{pmatrix}_{\text{logical}} \Leftrightarrow \begin{pmatrix}|0,0,0\rangle\\|0,1,1\rangle\\|1,0,1\rangle\\|1,1,0\rangle\end{pmatrix}^{\text{even}}_{\text{physical}}. \quad \text{(A30)}$$

In the logical qubit basis, the braiding operators are represented as

$$\begin{aligned}\mathcal{B}_1 &\simeq e^{-i\pi/4}\text{diag}(1, i, i, 1),\\ \mathcal{B}_2 &\simeq I_2 \otimes R_x,\\ \mathcal{B}_3 &\simeq e^{-i\pi/4}\text{diag}(1, i, 1, i),\\ \mathcal{B}_4 &\simeq U_{xx},\\ \mathcal{B}_5 &\simeq e^{-i\pi/4}\text{diag}(1, 1, i, i),\end{aligned} \quad \text{(A31)}$$

where $R_x$ is defined by (A16) and $U_{xx}$ is defined by (A15).

### *a. Pauli gates*

The two-qubit Pauli gates are defined by

$$\sigma_{k_2} \otimes \sigma_{k_1}, \quad \text{(A32)}$$

where $k_1$ and $k_2$ take 0, $x$, $y$, and $z$. The Pauli Z gates are generated by braiding $\mathcal{B}_{2k+1}$ with odd indices,

$$I_2 \otimes \sigma_Z \simeq i\mathcal{B}_3^2, \quad \sigma_Z \otimes I_2 \simeq i\mathcal{B}_5^2, \quad \sigma_Z \otimes \sigma_Z \simeq -\mathcal{B}_5^2\mathcal{B}_3^2. \quad \text{(A33)}$$

They are summarized as

$$(\sigma_Z)^{n_2} \otimes (\sigma_Z)^{n_1} \simeq \left(i\mathcal{B}_5^2\right)^{n_2}\left(i\mathcal{B}_3^2\right)^{n_1}, \quad \text{(A34)}$$

where $n_1$ and $n_2$ take 0 or 1.

The Pauli X gates are generated by braiding with even indices $\mathcal{B}_{2k}$,

$$I_2 \otimes \sigma_X \simeq i\mathcal{B}_2^2, \quad \sigma_X \otimes \sigma_X \simeq i\mathcal{B}_4^2, \quad I_2 \otimes \sigma_X \simeq -\mathcal{B}_4^2\mathcal{B}_2^2. \quad \text{(A35)}$$

It should be noted that $\mathcal{B}_4^2$ does not generate $I_2 \otimes \sigma_X$ but generates $\sigma_X \otimes \sigma_X$. We show the braiding for Pauli gates in Fig. 4.

Pauli Y gates are generated by sequential applications of Pauli X gates and Pauli Z gates based on the relation $U_Y = iU_XU_Z$ . Thus, all of Pauli gates for two qubits can be generated by braiding.

### *b. Hadamard gates*

The Hadamard gate acting on the first qubit can be embedded as

$$I_2 \otimes U_H \simeq i\mathcal{B}_2\mathcal{B}_3\mathcal{B}_2. \quad \text{(A36)}$$

The Hadamard gate acting on the second qubit can be embedded as

$$U_H \otimes I_2 \simeq -\mathcal{B}_1\mathcal{B}_2\mathcal{B}_3\mathcal{B}_4\mathcal{B}_3\mathcal{B}_2\mathcal{B}_1. \quad \text{(A37)}$$

These correspond to Eq. (21) in the main text. It requires more braiding than the previous results [46,50], where three braiding are enough. It is due to the choice of the correspondence between the physical and logical qubits.

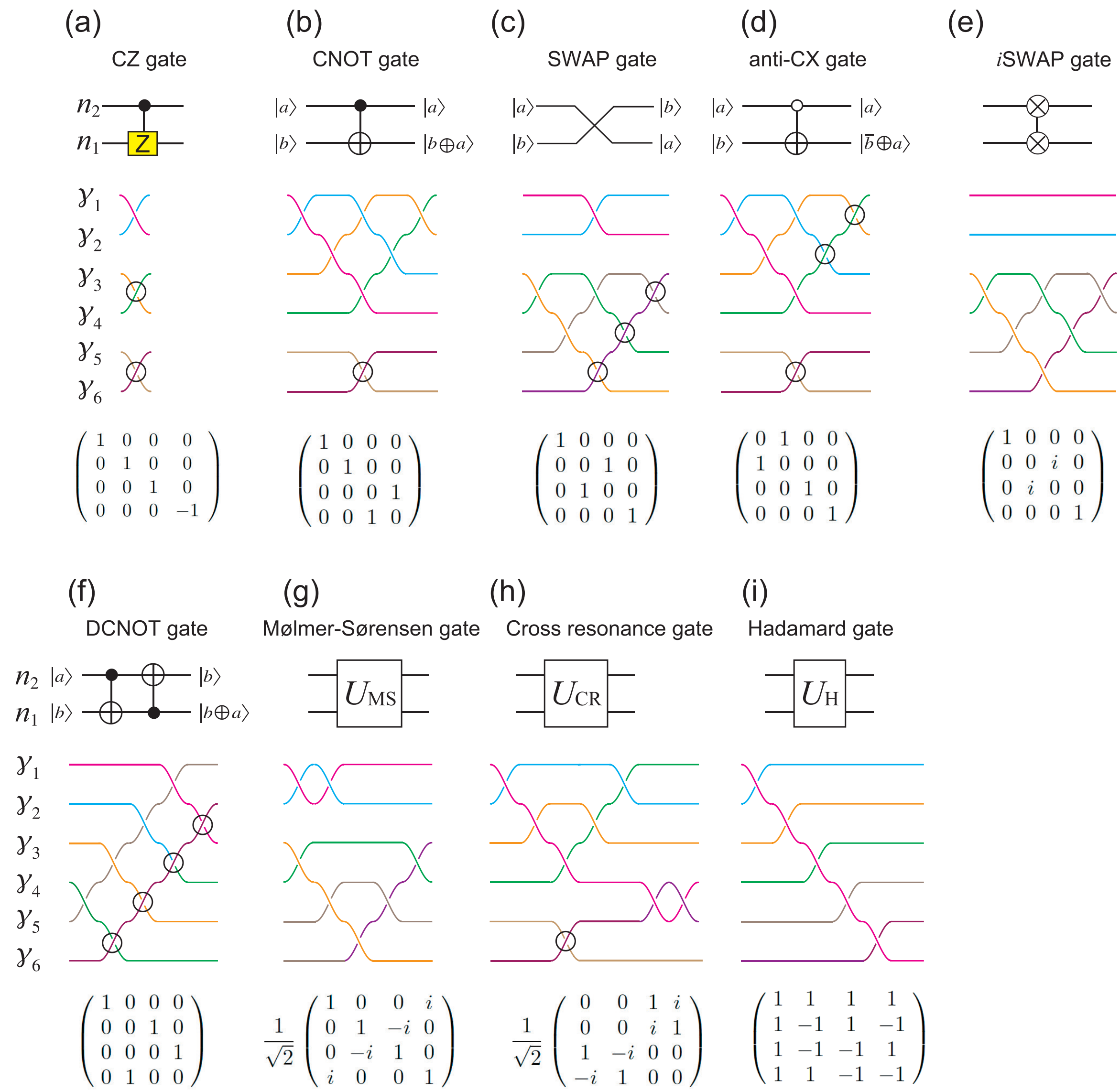


FIG. 5. Braiding process for various two-qubit quantum gates. (a) CZ gate, (b) CNOT gate, (c) SWAP gate, (d) anti-CX gate, (e) *i*SWAP gate, (f) DCNOT gate, (g) Molmer-Sorensen gate, (h) cross-resonance gate, and (i) Hadamard gate.

#### *c. Quantum gates for two logical qubits*

It is known that the controlled-Z (CZ) gate

$$U_{\mathrm{CZ}} = \mathrm{diag}(1, 1, 1, -1) \tag{A38}$$

is generated as [46]

$$U_{\mathrm{CZ}} \simeq e^{-i\pi/4}\mathcal{B}_5^{-1}(\mathcal{B}_3)^{-1}\mathcal{B}_1. \tag{A39}$$

See Fig. 5(a).

It is also known that the controlled-NOT (CNOT) gate

$$U_{\mathrm{CNOT}} = \begin{pmatrix} 1 & 0 & 0 & 0 \\ 0 & 1 & 0 & 0 \\ 0 & 0 & 0 & 1 \\ 0 & 0 & 1 & 0 \end{pmatrix} \tag{A40}$$

is generated by seven braiding [31,45,46], where braiding are given by

$$U_{\mathrm{CNOT}} \simeq -e^{-i\pi/4}\mathcal{B}_5^{-1}\mathcal{B}_1\mathcal{B}_2\mathcal{B}_3\mathcal{B}_1\mathcal{B}_2\mathcal{B}_1. \tag{A41}$$

See Fig. 5(b). On the other hand, there is a quantum circuit decomposition formula,

$$U_{\mathrm{CNOT}} = (I_2 \otimes U_H)U_{\mathrm{CZ}}(I_2 \otimes U_H), \tag{A42}$$

which involves nine braiding.

The SWAP gate is defined by

$$U_{\mathrm{SWAP}} \equiv \begin{pmatrix} 1 & 0 & 0 & 0 \\ 0 & 0 & 1 & 0 \\ 0 & 1 & 0 & 0 \\ 0 & 0 & 0 & 1 \end{pmatrix}, \tag{A43}$$

which is realized by seven braiding as

$$U_{\mathrm{SWAP}} \simeq e^{i\pi/4}(\mathcal{B}_3)^{-1}(\mathcal{B}_4)^{-1}(\mathcal{B}_5)^{-1}\mathcal{B}_3\mathcal{B}_4\mathcal{B}_3\mathcal{B}_1. \tag{A44}$$

See Fig. 5(c). This is smaller than the previous result using 15 braiding [46] based on the quantum circuit decomposition,

$$U_{\mathrm{SWAP}}=(I_2\otimes U_H)U_{\mathrm{CZ}}(I_2\otimes U_H)(U_H\otimes I_2)U_{\mathrm{CZ}}(U_H\otimes I_2)(I_2\otimes U_H)U_{\mathrm{CZ}}(I_2\otimes U_H). \tag{A45}$$

We list up various quantum gates generated by braiding. The anti-CNOT gate is defined by [57]

$$U_{\overline{\mathrm{C}}\mathrm{X}}\equiv\begin{pmatrix}0&1&0&0\\1&0&0&0\\0&0&1&0\\0&0&0&1\end{pmatrix}, \tag{A46}$$

which is generated by seven braiding

$$U_{\overline{\mathrm{C}}\mathrm{X}}\simeq e^{i\pi/4}\mathcal{B}_5^{-1}\mathcal{B}_1^{-1}\mathcal{B}_2^{-1}\mathcal{B}_3\mathcal{B}_1\mathcal{B}_2\mathcal{B}_1. \tag{A47}$$

It can be decomposed into $U_{\overline{\mathrm{C}}\mathrm{X}}=(I_2\otimes U_X)U_{\mathrm{CNOT}}$. If we use this relation, then nine braiding are necessary. See Fig. 5(d).

The $i$SWAP gate is defined by

$$U_{i\mathrm{SWAP}}\equiv\begin{pmatrix}1&0&0&0\\0&0&i&0\\0&i&0&0\\0&0&0&1\end{pmatrix}, \tag{A48}$$

which is realized by the six braiding

$$U_{i\mathrm{SWAP}}\simeq-\mathcal{B}_3\mathcal{B}_4\mathcal{B}_5\mathcal{B}_3\mathcal{B}_4\mathcal{B}_3. \tag{A49}$$

See Fig. 5(e).

The double CNOT gate is defined by [58]

$$U_{\mathrm{DCNOT}}\equiv\begin{pmatrix}1&0&0&0\\0&0&1&0\\0&0&0&1\\0&1&0&0\end{pmatrix}, \tag{A50}$$

which is realized by

$$U_{\mathrm{DCNOT}}\simeq\mathcal{B}_2^{-1}\mathcal{B}_3^{-1}\mathcal{B}_4^{-1}\mathcal{B}_5^{-1}\mathcal{B}_1\mathcal{B}_2\mathcal{B}_3\mathcal{B}_4. \tag{A51}$$

See Fig. 5(f).

The Mølmer-Sørensen gate is defined by [59]

$$U_{\mathrm{MS}}\equiv\frac{1}{\sqrt{2}}\begin{pmatrix}1&0&0&i\\0&1&-i&0\\0&-i&1&0\\i&0&0&1\end{pmatrix}, \tag{A52}$$

which is realized by

$$U_{\mathrm{MS}}\simeq-i\mathcal{B}_3\mathcal{B}_4\mathcal{B}_5\mathcal{B}_4\mathcal{B}_3\mathcal{B}_1\mathcal{B}_1. \tag{A53}$$

See Fig. 5(g).

The cross-resonance gate is defined by [60]

$$U_{\mathrm{CR}}\equiv\frac{1}{\sqrt{2}}\begin{pmatrix}0&0&1&i\\0&0&i&1\\1&-i&0&0\\-i&1&0&0\end{pmatrix}, \tag{A54}$$

which is realized by

$$U_{\mathrm{CR}}\simeq-\mathcal{B}_4\mathcal{B}_4\mathcal{B}_1\mathcal{B}_2\mathcal{B}_3\mathcal{B}_2\mathcal{B}_1. \tag{A55}$$

See Fig. 5(h).

We define the entangled Hadamard gate by

$$U_H^{(2)}=\begin{pmatrix}1&1&1&1\\1&-1&1&-1\\1&-1&-1&1\\1&1&-1&-1\end{pmatrix}, \tag{A56}$$

which is realized by

$$U_H^{(2)}\simeq-e^{-i\pi/4}\mathcal{B}_5\mathcal{B}_4\mathcal{B}_3\mathcal{B}_2\mathcal{B}_1. \tag{A57}$$

See Fig. 5(i). It is different from the cross product of the Hadamard gates,

$$U_H^{(2)}\neq U_H\otimes U_H. \tag{A58}$$

We note that it is obtained by a permutation of the third and fourth columns of the cross product of the Hadamard gates given by

$$U_H\otimes U_H=\begin{pmatrix}1&1&1&1\\1&-1&1&-1\\1&1&-1&-1\\1&-1&-1&1\end{pmatrix}, \tag{A59}$$

which leads to a relation

$$U_H\otimes U_H=U_{\mathrm{CNOT}}U_H^{(2)}. \tag{A60}$$

Hence, it is realized by

$$U_H\otimes U_H\simeq-\mathcal{B}_5^{-1}\mathcal{B}_1\mathcal{B}_2\mathcal{B}_3\mathcal{B}_1\mathcal{B}_2\mathcal{B}_1\mathcal{B}_5\mathcal{B}_4\mathcal{B}_3\mathcal{B}_2\mathcal{B}_1. \tag{A61}$$

Both $U_H^{(2)}$ and $U_H\otimes U_H$ are the Hadamard gates and they are useful for various quantum algorithms.

### *d. Equal-coefficient states*

The equal-coefficient state is constructed as

$$\begin{aligned}&i\mathcal{B}_1\mathcal{B}_2\mathcal{B}_3\mathcal{B}_4\mathcal{B}_5|0,0\rangle_{\mathrm{logical}}\\&=\tfrac{1}{2}(|0,0\rangle_{\mathrm{logical}}+|0,1\rangle_{\mathrm{logical}}+|1,0\rangle_{\mathrm{logical}}+|1,1\rangle_{\mathrm{logical}})\\&\equiv\tfrac{1}{2}\left(|0\rangle_{\mathrm{logical}}^{\mathrm{decimal}}+|1\rangle_{\mathrm{logical}}^{\mathrm{decimal}}+|2\rangle_{\mathrm{logical}}^{\mathrm{decimal}}+|3\rangle_{\mathrm{logical}}^{\mathrm{decimal}}\right),\end{aligned} \tag{A62}$$

where $|j\rangle_{\mathrm{logical}}^{\mathrm{decimal}}$ is a decimal representation of qubits. It is a fundamental entangled state for two qubits.

### 4. Four physical qubits and three logical qubits

We use eight Majorana fermions to construct three logical qubits,

$$\begin{aligned}c_1&=\tfrac{1}{2}(\gamma_1+i\gamma_2),\quad c_2=\tfrac{1}{2}(\gamma_3+i\gamma_4),\\c_3&=\tfrac{1}{2}(\gamma_5+i\gamma_6).\quad c_4=\tfrac{1}{2}(\gamma_7+i\gamma_8).\end{aligned} \tag{A63}$$

The explicit braid actions on the physical qubits are

$$\mathcal{B}_1\simeq\exp\left[-i\frac{\pi}{4}I_8\otimes\sigma_z\right]=I_8U_{\mathrm{S}},$$

$$\mathcal{B}_2\simeq\exp\left[-i\frac{\pi}{4}I_4\otimes\sigma_x\otimes\sigma_x\right]=I_4U_{xx},$$

$$\mathcal{B}_3\simeq\exp\left[-i\frac{\pi}{4}I_4\otimes\sigma_z\otimes I_2\right]=I_4U_{\mathrm{S}}\otimes I_2,$$

$$\mathcal{B}_4\simeq\exp\left[-i\frac{\pi}{4}I_2\otimes\sigma_x\otimes\sigma_x\otimes I_2\right]=I_2\otimes U_{xx}\otimes I_2,$$

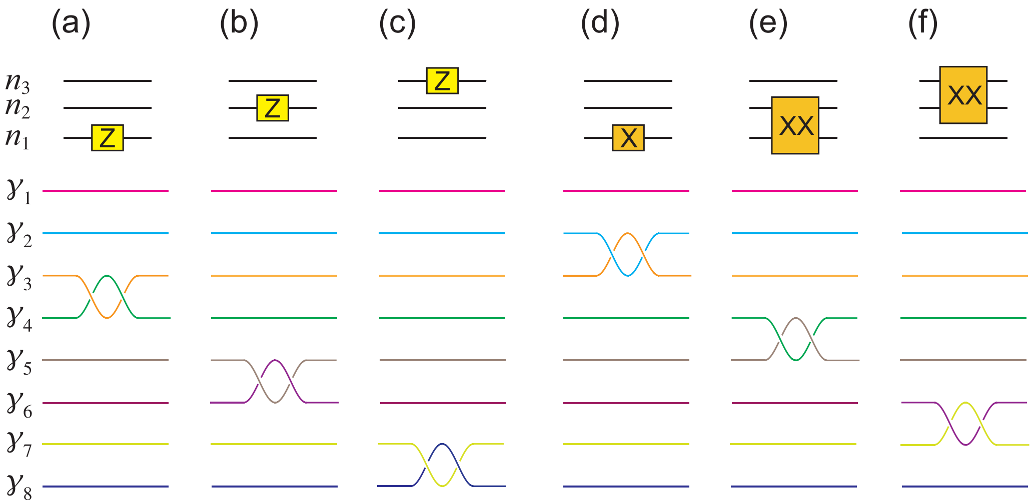


FIG. 6. Pauli gates embedded in three qubits. (a) Pauli Z gate embedded in the first qubit, (b) Pauli Z gate embedded in the second qubit, (c) Pauli Z gate embedded in the third qubit, (d) Pauli X gate embedded in the first qubit, (e) two Pauli X gates are embedded in the first and second qubits, and (f) Two Pauli X gates are embedded in the second third qubits.

$$\mathcal{B}_5 \simeq \exp\left[-i\frac{\pi}{4}I_2 \otimes \sigma_z \otimes I_4\right] = I_2 \otimes U_S \otimes I_4,$$
$$\mathcal{B}_6 \simeq \exp\left[-i\frac{\pi}{4}\sigma_x \otimes \sigma_x \otimes I_4\right] = U_{xx} \otimes I_4,$$
$$\mathcal{B}_7 \simeq \exp\left[-i\frac{\pi}{4}\sigma_z \otimes I_8\right] = U_S \otimes I_8. \quad \text{(A64)}$$

Three logical qubits are constructed from four physical qubits as

$$\begin{pmatrix} |0,0,0\rangle \\ |0,0,1\rangle \\ |0,1,0\rangle \\ |0,1,1\rangle \\ |1,0,0\rangle \\ |1,0,1\rangle \\ |1,1,0\rangle \\ |1,1,1\rangle \end{pmatrix}_{\text{logical}} \Leftrightarrow \begin{pmatrix} |0,0,0,0\rangle \\ |0,0,1,1\rangle \\ |0,1,0,1\rangle \\ |0,1,1,0\rangle \\ |1,0,0,1\rangle \\ |1,0,1,0\rangle \\ |1,1,0,0\rangle \\ |1,1,1,1\rangle \end{pmatrix}^{\text{even}}_{\text{physical}}. \quad \text{(A65)}$$

Explicit matrix representations for the braiding operator are

$$\mathcal{B}_1 \simeq e^{-i\pi/4}\text{diag}(1, i, i, 1, i, 1, 1, i)$$
$$= \exp\left[-\frac{i\pi}{4}\sigma_z \otimes \sigma_z \otimes \sigma_z\right],$$
$$\mathcal{B}_2 \simeq I_4 \otimes R_x,$$
$$\mathcal{B}_3 \simeq e^{-i\pi/4}\text{diag}(1, i, 1, i, 1, i, 1, i) = e^{-i\pi/4}I_4 \otimes U_S,$$
$$\mathcal{B}_4 \simeq I_2 \otimes U_{xx},$$
$$\mathcal{B}_5 \simeq e^{-i\pi/4}\text{diag}(1, 1, i, i, 1, 1, i, i) = e^{-i\pi/4}I_2 \otimes U_S \otimes I_2,$$
$$\mathcal{B}_6 \simeq U_{xx} \otimes I_2,$$
$$\mathcal{B}_7 \simeq e^{-i\pi/4}\text{diag}(1, 1, 1, 1, i, i, i, i) = e^{-i\pi/4}U_S \otimes I_4. \quad \text{(A66)}$$

### *a. Pauli gates*

The three-qubit Pauli gates are defined by

$$\sigma_{k_3} \otimes \sigma_{k_2} \otimes \sigma_{k_1}, \quad \text{(A67)}$$

where $k_1$, $k_2$, and $k_3$ take 0, $x$, $y$, and $z$. The Pauli Z gates are generated by braiding operators $\mathcal{B}_{2k+1}$ with odd indices

$$I_2 \otimes I_2 \otimes \sigma_Z \Leftrightarrow i\mathcal{B}_3^2, \quad I_2 \otimes \sigma_Z \otimes I_2 \Leftrightarrow i\mathcal{B}_5^2,$$
$$\sigma_Z \otimes I_2 \otimes I_2 \Leftrightarrow i\mathcal{B}_7^2, \quad \text{(A68)}$$

They are summarized as

$$(\sigma_Z)^{n_3} \otimes (\sigma_Z)^{n_2} \otimes (\sigma_Z)^{n_1} \Leftrightarrow \left(i\mathcal{B}_7^2\right)^{n_3}\left(i\mathcal{B}_5^2\right)^{n_2}\left(i\mathcal{B}_3^2\right)^{n_1}, \quad \text{(A69)}$$

where $n_1$, $n_2$, and $n_3$ take 0 or 1.

The Pauli X gates are generated by braiding operators with even numbers,

$$I_2 \otimes I_2 \otimes \sigma_X \simeq i\mathcal{B}_2^2, \quad I_2 \otimes \sigma_X \otimes \sigma_X \simeq i\mathcal{B}_4^2,$$
$$\sigma_X \otimes \sigma_X \otimes I_2 \simeq i\mathcal{B}_6^2. \quad \text{(A70)}$$

We show the corresponding braiding in Fig. 6. It is impossible to construct logical gates corresponding to

$$I_2 \otimes \sigma_X \otimes I_2 \quad \text{and} \quad \sigma_X \otimes I_2 \otimes I_2 \quad \text{(A71)}$$

solely by braiding. This problem is solved by introducing many-body interactions of Majorana fermions as in Eq. (B37).

The other Pauli gates can be generated by sequential applications of the above Pauli gates.

### *b. Diagonal braiding*

We first search braiding operators for the quantum gates generated by odd double braiding,

$$U_{\text{diag}} \simeq \left(\mathcal{B}_7^2\right)^{n_3}\left(\mathcal{B}_5^2\right)^{n_2}\left(\mathcal{B}_3^2\right)^{n_1}. \quad \text{(A72)}$$

There are eight patterns represented by the Pauli Z gates,

$$\text{diag}(1, 1, 1, 1, 1, 1, 1, 1) \simeq I_2 \otimes I_2 \otimes I_2,$$
$$\text{diag}(1, -1, 1, -1, 1, -1, 1, -1) \simeq I_2 \otimes I_2 \otimes \sigma_Z \Leftrightarrow i\mathcal{B}_3^2,$$
$$\text{diag}(1, 1, -1, -1, 1, 1, -1, -1) \simeq I_2 \otimes \sigma_Z \otimes I_2 \Leftrightarrow i\mathcal{B}_5^2,$$
$$\text{diag}(1, 1, 1, 1, -1, -1, -1, -1) \simeq \sigma_Z \otimes I_2 \otimes I_2 \Leftrightarrow i\mathcal{B}_7^2,$$
$$\text{diag}(1, -1, -1, 1, 1, -1, -1, 1) \simeq I_2 \otimes \sigma_Z \otimes \sigma_Z \Leftrightarrow -\mathcal{B}_5^2\mathcal{B}_3^2,$$

$$\begin{aligned}
&\mathrm{diag}(1,1,-1,-1,-1,-1,1,1) \simeq \sigma_Z \otimes \sigma_Z \otimes I_2 \Leftrightarrow -\mathcal{B}_7^2\mathcal{B}_5^2,\\
&\mathrm{diag}(1,-1,1,-1,-1,1,-1,1) \simeq \sigma_Z \otimes I_2 \otimes \sigma_Z \Leftrightarrow -\mathcal{B}_7^2\mathcal{B}_3^2,\\
&\mathrm{diag}(1,-1,-1,1,-1,1,1,-1) \simeq \sigma_Z \otimes \sigma_Z \otimes \sigma_Z\\
&\qquad \Leftrightarrow -i\mathcal{B}_7^2\mathcal{B}_5^2\mathcal{B}_3^2. \qquad \text{(A73)}
\end{aligned}$$

Next, we search real and diagonal gates obtained by the following odd braiding:

$$(\mathcal{B}_7)^{n_3}(\mathcal{B}_5)^{n_2}(\mathcal{B}_3)^{n_1}. \qquad \text{(A74)}$$

We search states whose components are $\pm 1$. There are four additional quantum gates, whose traces are zero $\mathrm{Tr}U_{\mathrm{diag}} = 0$,

$$\begin{aligned}
&\mathrm{diag}(1,-1,-1,-1,1,1,1,-1) \Leftrightarrow i\mathcal{B}_4^{-1}\mathcal{B}_3\mathcal{B}_2\mathcal{B}_1,\\
&\mathrm{diag}(1,-1,1,1,-1,-1,1,-1) \Leftrightarrow i\mathcal{B}_3^{-1}\mathcal{B}_4\mathcal{B}_2\mathcal{B}_1,\\
&\mathrm{diag}(1,1,-1,1,-1,1,-1,-1) \Leftrightarrow i\mathcal{B}_2^{-1}\mathcal{B}_3\mathcal{B}_4\mathcal{B}_1,\\
&\mathrm{diag}(1,1,1,-1,1,-1,-1,-1) \Leftrightarrow -i\mathcal{B}_4^{-1}\mathcal{B}_3^{-1}\mathcal{B}_2^{-1}\mathcal{B}_1. \qquad \text{(A75)}
\end{aligned}$$

In addition, there are additional quantum gates, whose traces are nonzero $\mathrm{Tr}U_{\mathrm{diag}} \neq 0$,

$$\begin{aligned}
&\mathrm{diag}(1,-1,-1,-1,-1,-1,-1,1) \simeq -\mathcal{B}_4\mathcal{B}_3\mathcal{B}_2\mathcal{B}_1,\\
&\mathrm{diag}(1,-1,1,1,1,1,-1,1) \simeq \mathcal{B}_4^{-1}\mathcal{B}_3^{-1}\mathcal{B}_2\mathcal{B}_1,\\
&\mathrm{diag}(1,1,-1,1,1,-1,1,1) \simeq \mathcal{B}_4^{-1}\mathcal{B}_2^{-1}\mathcal{B}_3\mathcal{B}_1,\\
&\mathrm{diag}(1,1,1,-1,-1,1,1,1) \simeq \mathcal{B}_3^{-1}\mathcal{B}_2^{-1}\mathcal{B}_4\mathcal{B}_1. \qquad \text{(A76)}
\end{aligned}$$

It is natural to anticipate that the CZ gate and the CCZ gate are generated by even braiding because they are diagonal gates. However, this is not the case by checking all $4^3$ patterns of braiding. As a result, the even braiding do not generate the CZ gates,

$$\begin{aligned}
I_2 \otimes U_{\mathrm{CZ}} &= \mathrm{diag}(1,1,1,-1,1,1,1,-1),\\
U_{\mathrm{CZ}} \otimes I_2 &= \mathrm{diag}(1,1,1,1,1,1,-1,-1), \qquad \text{(A77)}
\end{aligned}$$

and the CCZ gate,

$$U_{\mathrm{CCZ}} = \mathrm{diag}(1,1,1,1,1,1,1,-1). \qquad \text{(A78)}$$

This problem is solved by introducing many-body interactions of Majorana fermions as shown in the main text.

#### c. Hadamard gates

The Hadamard gate can be embedded in the first qubit as

$$I_2 \otimes I_2 \otimes U_H \simeq i\mathcal{B}_2\mathcal{B}_3\mathcal{B}_2, \qquad \text{(A79)}$$

as in the case of (A36). We also find that the Hadamard gate can be embedded in the third qubit as

$$U_H \otimes I_2 \otimes I_2 \simeq -i\mathcal{B}_1\mathcal{B}_2\mathcal{B}_3\mathcal{B}_4\mathcal{B}_5\mathcal{B}_6\mathcal{B}_5\mathcal{B}_4\mathcal{B}_3\mathcal{B}_2\mathcal{B}_1. \qquad \text{(A80)}$$

These correspond to Eq. (21) in the main text. On the other hand, it is hard to embed the Hadamard gate in the second qubit $I_2 \otimes U_H \otimes I_2$. It is possible by introducing many-body interactions of Majorana fermions. The Hadamard gate for the $N$th qubit is given by

$$U_H \otimes I_{2N-2} \simeq \mathcal{B}_1\mathcal{B}_2\cdots\mathcal{B}_{2N-1}\mathcal{B}_{2N}\mathcal{B}_{2N-1}\cdots\mathcal{B}_2\mathcal{B}_1 \qquad \text{(A81)}$$

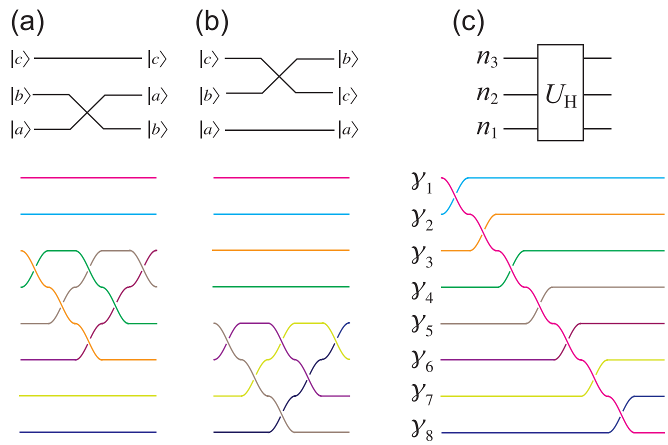


FIG. 7. [(a) and (b)] $i$SWAP gate embedded in three-qubit systems. (c) Three-qubit Hadamard transformation.

up to a phase factor.

#### d. Two-qubit quantum gates embedded in three-qubit quantum gates

The $i$SWAP gate can be embedded in a three-qubit topological gate because it does not involve $\mathcal{B}_1$ and is given by

$$I_2 \otimes U_{i\mathrm{SWAP}} \simeq -\mathcal{B}_3\mathcal{B}_4\mathcal{B}_5\mathcal{B}_3\mathcal{B}_4\mathcal{B}_3. \qquad \text{(A82)}$$

See Fig. 7(a). We also find the $i$SWAP gate can be embedded as

$$U_{i\mathrm{SWAP}} \otimes I_2 \simeq -\mathcal{B}_5\mathcal{B}_6\mathcal{B}_7\mathcal{B}_5\mathcal{B}_6\mathcal{B}_5. \qquad \text{(A83)}$$

See Fig. 7(b).

#### e. Three-qubit quantum gates

We find that the three-qubit Hadamard transformation is generated as

$$U_H^{(3)} = \begin{pmatrix}
1 & 1 & 1 & 1 & 1 & 1 & 1 & 1\\
1 & -1 & 1 & -1 & 1 & -1 & 1 & -1\\
1 & -1 & -1 & 1 & 1 & -1 & -1 & 1\\
1 & 1 & -1 & -1 & 1 & 1 & -1 & -1\\
1 & -1 & -1 & 1 & -1 & 1 & 1 & -1\\
1 & 1 & -1 & -1 & -1 & -1 & 1 & 1\\
1 & 1 & 1 & 1 & -1 & -1 & -1 & -1\\
1 & -1 & 1 & -1 & -1 & 1 & -1 & 1
\end{pmatrix}$$
$$\simeq -\mathcal{B}_7\mathcal{B}_6\mathcal{B}_5\mathcal{B}_4\mathcal{B}_3\mathcal{B}_2\mathcal{B}_1. \qquad \text{(A84)}$$

See Fig. 7(b). It is different from the cross product of the Hadamard gate,

$$U_H \otimes U_H \otimes U_H$$
$$= \begin{pmatrix}
1 & 1 & 1 & 1 & 1 & 1 & 1 & 1\\
1 & -1 & 1 & -1 & 1 & -1 & 1 & -1\\
1 & 1 & -1 & -1 & 1 & 1 & -1 & -1\\
1 & -1 & -1 & 1 & 1 & -1 & -1 & 1\\
1 & 1 & 1 & 1 & -1 & -1 & -1 & -1\\
1 & -1 & 1 & -1 & -1 & 1 & -1 & 1\\
1 & 1 & -1 & -1 & -1 & -1 & 1 & 1\\
1 & -1 & -1 & 1 & -1 & 1 & 1 & -1
\end{pmatrix}. \qquad \text{(A85)}$$

There is a relation

$$U_H \otimes U_H \otimes U_H = -U_{3P} U_H^{(3)}, \tag{A86}$$

where $U_{3P}$ is defined by

$$U \equiv \begin{pmatrix} 1 & 0 & 0 & 0 & 0 & 0 & 0 & 0 \\ 0 & 1 & 0 & 0 & 0 & 0 & 0 & 0 \\ 0 & 0 & 0 & 1 & 0 & 0 & 0 & 0 \\ 0 & 0 & 1 & 0 & 0 & 0 & 0 & 0 \\ 0 & 0 & 0 & 0 & 0 & 0 & 1 & 0 \\ 0 & 0 & 0 & 0 & 0 & 0 & 0 & 1 \\ 0 & 0 & 0 & 0 & 0 & 1 & 0 & 0 \\ 0 & 0 & 0 & 0 & 1 & 0 & 0 & 0 \end{pmatrix}. \tag{A87}$$

It is impossible to generate the W state by braiding

$$|\mathrm{W}\rangle_{\text{logical}} = \frac{1}{\sqrt{3}}(|000\rangle_{\text{logical}} + |010\rangle_{\text{logical}} + |100\rangle_{\text{logical}}), \tag{A88}$$

because the number of the nonzero terms of the W state is 3, which contradicts the fact that the number of the nonzero terms must be 1, 2, 4, and 8 for three-qubit states generated by braiding.

#### *f. Embedding problem of the CZ gate*

The CZ gate is given by the braiding $e^{-i\pi/4}\mathcal{B}_5^{-1}(\mathcal{B}_3)^{-1}\mathcal{B}_1$ for two logical qubits, whose matrix representation is

$$\text{diag}(1, 1, 1, -1, i, -i, -i, -i), \tag{A89}$$

once it is embedded in three logical qubits. They are different,

$$e^{-i\pi/4}\mathcal{B}_5^{-1}(\mathcal{B}_3)^{-1}\mathcal{B}_1 \neq I_2 \otimes U_{\text{CZ}} = \text{diag}(1, 1, 1, -1, 1, 1, 1, -1). \tag{A90}$$

In general, $M$-quantum gates cannot be embedded in $N$ qubit. We solve the problem by introducing many-body interaction of Majorana fermions in Eq. (26) in the main text

### 5. $N$ logical qubits

The braid representation of $2N + 2$ Majorana fermions is equivalent to the $\pi/2$ rotation in SO($2N + 2$), suggested by the fact that braid operators are represented by the Gamma matrices [47,48]. The number of the braid group is given by [19]

$$|\text{Image}(\mathcal{B}_{2n})| = \begin{cases} 2^{2n-1}(2n)! & \text{for} \quad n\text{=even} \\ 2^{2n}(2n)! & \text{for} \quad n\text{=odd} \end{cases}. \tag{A91}$$

The $i$SWAP gate is embedded as

$$I_2^{k-2} \otimes U_{i\text{SWAP}} \otimes I_2^{N-k} \simeq \mathcal{B}_{2k+1}\mathcal{B}_{2k+2}\mathcal{B}_{2k+3}\mathcal{B}_{2k+1}\mathcal{B}_{2k+2}\mathcal{B}_{2k+1} \tag{A92}$$

up to a phase factor.

#### *a. Diagonal braiding*

We consider odd braiding defined by

$$\mathcal{B}_{\text{odd}}(n_1, n_2, \ldots, n_k) \equiv \mathcal{B}_{2n_k-1}\mathcal{B}_{2n_{k-1}-1}\cdots\mathcal{B}_{2n_1-1}, \tag{A93}$$

where $n_k$ is an integer satisfying $1 \leqslant n_k \leqslant N + 1$. They are Abelian braiding because there are no adjacent braiding. Then, there are only $4^k$ patterns. Especially, we consider odd double braiding defined by

$$(\mathcal{B}_{\text{odd}})^2 \equiv \left(i\mathcal{B}^2_{2n_k-1}\right)\left(i\mathcal{B}^2_{2n_{k-1}-1}\right)\cdots\left(i\mathcal{B}^2_{2n_1-1}\right) \tag{A94}$$

are interesting because they are identical to

$$(\mathcal{B}_{\text{odd}})^2 \simeq (\sigma_Z)^{m_k}(\sigma_Z)^{m_2}\cdots(\sigma_Z)^{m_1}, \tag{A95}$$

where $m_k = 0, 1$. Namely every Pauli gates constructing from the Pauli Z gate can be generated.

Next, we consider even braiding defined by

$$\mathcal{B}_{\text{even}}(n_1, n_2, \ldots, n_k) \equiv \mathcal{B}_{2n_k}\mathcal{B}_{2n_{k-1}}\cdots\mathcal{B}_{2n_1}. \tag{A96}$$

They are also the Abelian braiding, where each braiding commutes each other. We also consider even double braiding defined by

$$(\mathcal{B}_{\text{even}})^2 \equiv \left(i\mathcal{B}^2_{2n_k}\right)\left(i\mathcal{B}^2_{2n_{k-1}}\right)\cdots\left(i\mathcal{B}^2_{2n_1}\right). \tag{A97}$$

On the other hand, it is impossible to construct the Pauli X gate except for the first qubit.

#### *b. Hadamard transformation*

The Hadamard transformation is used for the initial process of various quantum algorithm such as the Kitaev phase estimation algorithm, the Deutsch algorithm, the Deutsch-Jozsa algorithm, the Simon algorithm, the Bernstein-Vazirani algorithm, the Grover algorithm, and the Shor algorithm. It is generated by the braiding

$$U_H^{(N)} \simeq \mathcal{B}_{2N+1}\mathcal{B}_{2N}\cdots\mathcal{B}_2\mathcal{B}_1, \tag{A98}$$

up to a phase factor. The equal-coefficient state is generated as

$$U_H^{(N)}|0, 0\rangle_{\text{logical}} \propto \sum_{j=1}^{2^N} |j\rangle_{\text{logical}}, \tag{A99}$$

where $|j\rangle_{\text{logical}}$ is the decimal representation of the qubit.

## APPENDIX B: 2$N$-BODY UNITARY EVOLUTION

### 1. Quantum gates for one logical qubit

The two-body Majorana operator $\mathcal{B}_1(\theta)$ is written in terms of fermion operators,

$$\mathcal{B}_1(\theta) = \cos\theta + \gamma_2\gamma_1\sin\theta = [\cos\theta + (ic_1^\dagger c_1 - ic_1c_1^\dagger)\sin\theta], \tag{B1}$$

which operates on two physical qubits (A3) as

$$\mathcal{B}_1(\theta)|\Psi_1\rangle_{\text{physical}} = \begin{pmatrix} e^{-i\theta} & 0 & 0 & 0 \\ 0 & e^{i\theta} & 0 & 0 \\ 0 & 0 & e^{-i\theta} & 0 \\ 0 & 0 & 0 & e^{i\theta} \end{pmatrix} \begin{pmatrix} |0,0\rangle \\ |0,1\rangle \\ |1,0\rangle \\ |1,1\rangle \end{pmatrix}_{\text{physical}}. \tag{B2}$$

Taking the even-parity basis, the action is

$$\mathcal{B}_1(\theta)|\Psi_1\rangle^{\text{even}}_{\text{physical}} = e^{-i\theta}\begin{pmatrix} 1 & 0 \\ 0 & e^{2i\theta} \end{pmatrix}\begin{pmatrix} |0\rangle \\ |1\rangle \end{pmatrix}_{\text{logical}}. \tag{B3}$$

It is the arbitrary phase-shift gate. Especially, by setting $\theta = \pi/8$, the T gate is constructed as

$$U_T \equiv \mathrm{diag}(1, e^{i\pi/4}). \quad \text{(B4)}$$

It is identical to the rotation along the $z$ axis,

$$\mathcal{B}_1(\theta) \simeq R_z(2\theta), \quad \text{(B5)}$$

with

$$R_z(\theta) \equiv \exp\left[-i\frac{\theta}{2}\sigma_z\right] = \begin{pmatrix} e^{-i\theta/2} & 0 \\ 0 & e^{i\theta/2} \end{pmatrix}. \quad \text{(B6)}$$

The operator $\mathcal{B}_2$ is written in terms of fermion operators,

$$\begin{aligned}\mathcal{B}_2(\theta) &= \cos\theta + \gamma_3\gamma_2 \sin\theta \\ &= \cos\theta + (ic_2c_1^\dagger + ic_2^\dagger c_1^\dagger - ic_2c_1 - ic_2^\dagger c_1)\sin\theta, \end{aligned} \quad \text{(B7)}$$

which operates on two physical qubits (A3) as [14],

$$\mathcal{B}_2(\theta)\Psi_{\text{physical}} = \begin{pmatrix} \cos\theta & 0 & 0 & -i\sin\theta \\ 0 & \cos\theta & -i\sin\theta & 0 \\ 0 & -i\sin\theta & \cos\theta & 0 \\ -i\sin\theta & 0 & 0 & \cos\theta \end{pmatrix} \begin{pmatrix} |0,0\rangle \\ |0,1\rangle \\ |1,0\rangle \\ |1,1\rangle \end{pmatrix}_{\text{physical}}. \quad \text{(B8)}$$

In the even-parity basis, the action is

$$\mathcal{B}_2(\theta) = \begin{pmatrix} \cos\theta & -i\sin\theta \\ -i\sin\theta & \cos\theta \end{pmatrix} \equiv R_x(2\theta), \quad \text{(B9)}$$

which is identical to the rotation along the $x$ axis,

$$\mathcal{B}_2(\theta) = R_x(2\theta), \quad \text{(B10)}$$

with

$$R_x(\theta) \equiv \exp\left[-i\frac{\theta}{2}\sigma_x\right] = \begin{pmatrix} \cos\frac{\theta}{2} & -i\sin\frac{\theta}{2} \\ -i\sin\frac{\theta}{2} & \cos\frac{\theta}{2} \end{pmatrix}. \quad \text{(B11)}$$

The operator $\mathcal{B}_3(\theta)$ is written in terms of fermion operators

$$\mathcal{B}_3(\theta) = \cos\theta + \gamma_4\gamma_3 \sin\theta = \cos\theta + (ic_2^\dagger c_2 - ic_2c_2^\dagger)\sin\theta, \quad \text{(B12)}$$

which operates on two physical qubits (A3) as [14]

$$\mathcal{B}_3(\theta)|\Psi_1\rangle_{\text{physical}} = \begin{pmatrix} e^{-i\theta} & 0 & 0 & 0 \\ 0 & e^{-i\theta} & 0 & 0 \\ 0 & 0 & e^{i\theta} & 0 \\ 0 & 0 & 0 & e^{i\theta} \end{pmatrix} \begin{pmatrix} |0,0\rangle \\ |0,1\rangle \\ |1,0\rangle \\ |1,1\rangle \end{pmatrix}_{\text{physical}}. \quad \text{(B13)}$$

In the even-parity basis, the action is the same as (B3),

$$\mathcal{B}_3(\theta)|\Psi_1\rangle^{\text{even}}_{\text{physical}} = e^{-i\theta}\begin{pmatrix} 1 & 0 \\ 0 & e^{2i\theta} \end{pmatrix}\begin{pmatrix} |0\rangle \\ |1\rangle \end{pmatrix}_{\text{logical}}. \quad \text{(B14)}$$

The rotation along the $y$ axis is defined by

$$R_y(\theta) \equiv \exp\left[-i\frac{\theta}{2}\sigma_y\right], \quad \text{(B15)}$$

and is realized by the sequential operations

$$R_y(\theta) = R_z\left(\frac{\pi}{2}\right)R_x(\theta)R_z\left(-\frac{\pi}{2}\right). \quad \text{(B16)}$$

### 2. Three physical qubits

Next we study the six Majorana fermion system. The explicit actions on the physical qubits are

$$\begin{aligned} \mathcal{B}_1(\theta) &\simeq \exp[-i\theta I_4 \otimes \sigma_z] = I_2 \otimes I_2 \otimes R_z(2\theta), \\ \mathcal{B}_2(\theta) &\simeq \exp[-i\theta I_2 \otimes \sigma_x \otimes \sigma_x] = I_2 \otimes U_{xx}(\theta), \\ \mathcal{B}_3(\theta) &\simeq \exp[-i\theta I_2 \otimes \sigma_z \otimes I_2] = I_2 \otimes R_z(2\theta) \otimes I_2, \\ \mathcal{B}_4(\theta) &\simeq \exp[-i\theta \sigma_x \otimes \sigma_x \otimes I_2] = U_{xx} \otimes I_2, \\ \mathcal{B}_5(\theta) &\simeq \exp[-i\theta \sigma_z \otimes I_4] = R_z(2\theta) \otimes I_4. \end{aligned} \quad \text{(B17)}$$

### 3. Two logical qubits

Two logical qubits are constructed from three physical qubits by taking the even-parity basis. The action of $\mathcal{B}_1(\theta)$ to the logical qubit is

$$\mathcal{B}_1(\theta) \simeq \mathrm{diag}(e^{-i\theta}, e^{i\theta}, e^{i\theta}, e^{-i\theta}), \quad \text{(B18)}$$

which is identical to the ZZ interaction

$$\mathcal{B}_1(\theta) \simeq U_{zz}(2\theta), \quad \text{(B19)}$$

with

$$U_{zz}(\theta) \equiv \exp\left[-i\frac{\theta}{2}\sigma_z \otimes \sigma_z\right]. \quad \text{(B20)}$$

The action of $\mathcal{B}_4(\theta)$ on the logical qubit is

$$\mathcal{B}_4(\theta) \simeq \begin{pmatrix} \cos\theta & 0 & 0 & -i\sin\theta \\ 0 & \cos\theta & -i\sin\theta & 0 \\ 0 & -i\sin\theta & \cos\theta & 0 \\ -i\sin\theta & 0 & 0 & \cos\theta \end{pmatrix}, \quad \text{(B21)}$$

which is identical to the $xx$ interaction

$$\mathcal{B}_4(\theta) \simeq U_{xx}(2\theta), \quad \text{(B22)}$$

with

$$U_{xx}(\theta) \equiv \exp\left[-i\frac{\theta}{2}\sigma_x \otimes \sigma_x\right]. \quad \text{(B23)}$$

The action of $\mathcal{B}_3(\theta)$ and $\mathcal{B}_5(\theta)$ on the logical qubit is

$$\begin{aligned} \mathcal{B}_3(\theta) &\simeq \mathrm{diag}(e^{-i\theta}, e^{i\theta}, e^{-i\theta}, e^{i\theta}) = I_2 \otimes U_z(\theta), \\ \mathcal{B}_5(\theta) &\simeq \mathrm{diag}(e^{-i\theta}, e^{-i\theta}, e^{i\theta}, e^{i\theta}) = U_z(\theta) \otimes I_2. \end{aligned} \quad \text{(B24)}$$

The action of $\mathcal{B}_2(\theta)$ on the logical qubit is

$$\mathcal{B}_2(\theta) \simeq \begin{pmatrix} \cos\theta & -i\sin\theta & 0 & 0 \\ -i\sin\theta & \cos\theta & 0 & 0 \\ 0 & 0 & \cos\theta & -i\sin\theta \\ 0 & 0 & -i\sin\theta & \cos\theta \end{pmatrix}, \quad \text{(B25)}$$

which is rewritten in the form of

$$\begin{aligned} \mathcal{B}_2(\theta) &\simeq I_2 \otimes R_x(2\theta), \\ \mathcal{B}_{2345}(\theta) &\simeq R_x(2\theta) \otimes I_2. \end{aligned} \quad \text{(B26)}$$

#### *a. Controlled phase-shift gate*

We find

$$\mathcal{B}_6(\theta_3)\mathcal{B}_3(\theta_2)\mathcal{B}_1(\theta_1) \simeq \mathrm{diag}(e^{-i(\theta_1+\theta_2+\theta_3)}, e^{i(\theta_1+\theta_2-\theta_3)}, e^{i(\theta_1-\theta_2+\theta_3)}, e^{i(-\theta_1+\theta_2+\theta_3)}). \tag{B27}$$

The controlled phase-shift gate with an arbitrary phase is constructed by setting $\theta_1 = -\theta_2 = -\theta_3 = -\theta$,

$$\mathcal{B}_5(-\theta)\mathcal{B}_3(\theta)\mathcal{B}_1(\theta) \simeq \mathrm{diag}(e^{-i\theta}, e^{-i\theta}, e^{-i\theta}, e^{3i\theta}) = e^{-i\theta}\mathrm{diag}(1, 1, 1, e^{4i\theta}). \tag{B28}$$

Especially, the CZ gate is constructed by setting $\theta = \pi/4$.

#### *b. Controlled-unitary gate*

It is known that the controlled unitary gate is constructed as [61]

$$U_{\text{C-}U} = (I_2 \otimes U_A)U_{\text{CNOT}}(I_2 \otimes U_B)U_{\text{CNOT}}(I_2 \otimes U_C) \tag{B29}$$

with

$$U_A \equiv R_z(\beta)R_y\left(\frac{\gamma}{2}\right), \quad U_B \equiv R_y\left(-\frac{\gamma}{2}\right)R_z\left(-\frac{\beta+\delta}{2}\right), \quad U_C \equiv R_z\left(\frac{\delta-\beta}{2}\right), \tag{B30}$$

because

$$U_AU_BU_C = I_4 \tag{B31}$$

and

$$U_AXU_BXU_C = R_z(\beta)R_y(\gamma)R_z(\delta) = U_{1\text{bit}}. \tag{B32}$$

In the Majorana system, the basic rotations are not along the $y$ axis but the $x$ axis. The similar decomposition is possible only by using the rotations along the $z$ and $x$ axes as

$$U_A = R_z\left(\beta+\frac{\pi}{2}\right)R_x\left(\frac{\gamma}{2}\right), \quad U_B = R_x\left(-\frac{\gamma}{2}\right)R_z\left(-\frac{\beta+\delta}{2}\right), \quad U_C = R_z\left(\frac{\delta-\beta-\pi}{2}\right). \tag{B33}$$

The proof is similar. First, we have

$$U_AU_BU_C = 1,$$

where we have used the relation

$$R_j(\theta_1)R_j(\theta_2) = R_j(\theta_1+\theta_2) \tag{B34}$$

for $j = x, y$, and $z$. Next, we have

$$U_AXU_BXU_C = U_{1\text{bit}},$$

where we have used the relation

$$R(\theta)X = XR(-\theta). \tag{B35}$$

Hence, the controlled unitary gate is implemented by two-body Majorana interaction.

### 4. Four physical qubits

We consider eight Majorana fermion system. The explicit actions on four physical qubits are given by

$$\begin{aligned}
\mathcal{B}_1 &\simeq I_8 \otimes R_z(2\theta),\\
\mathcal{B}_2 &\simeq I_4 \otimes U_{xx}(\theta),\\
\mathcal{B}_3 &\simeq I_4 \otimes R_z(2\theta) \otimes I_2,\\
\mathcal{B}_4 &\simeq I_2 \otimes U_{xx}(\theta) \otimes I_2,\\
\mathcal{B}_5 &\simeq I_2 \otimes R_z(2\theta) \otimes I_4,\\
\mathcal{B}_6 &\simeq U_{xx}(\theta) \otimes I_4,\\
\mathcal{B}_7 &\simeq R_z(2\theta) \otimes I_8,
\end{aligned} \tag{B36}$$

where $R_z$ is defined in (B6) and $U_{xx}$ is defined in (B23). We summarize results on constructing full set of Pauli Z gate for three logical qubits in the following table:

| | Four physical qubits | Three logical qubits |
|---|---|---|
| $\mathcal{B}_{12}(\theta)$ | $\exp[-i\theta I_8 \otimes \sigma_z]$ | $\exp[-i\theta\sigma_z \otimes \sigma_z \otimes \sigma_z]$ |
| $\mathcal{B}_{34}(\theta)$ | $\exp[-i\theta I_4 \otimes \sigma_z \otimes I_2]$ | $\exp[-i\theta I_4 \otimes \sigma_z]$ |
| $\mathcal{B}_{56}(\theta)$ | $\exp[-i\theta I_2 \otimes \sigma_z \otimes I_4]$ | $\exp[-i\theta I_2 \otimes \sigma_z \otimes I_2]$ |
| $\mathcal{B}_{78}(\theta)$ | $\exp[-i\theta\sigma_z \otimes I_8]$ | $\exp[-i\theta\sigma_z \otimes I_4]$ |
| $\mathcal{B}^{(4)}_{1234}(\theta)$ | $\exp[-i\theta I_4 \otimes \sigma_z \otimes \sigma_z]$ | $\exp[-i\theta\sigma_z \otimes \sigma_z \otimes I_2]$ |
| $\mathcal{B}^{(4)}_{1256}(\theta)$ | $\exp[-i\theta I_2 \otimes \sigma_z \otimes I_2 \otimes \sigma_z]$ | $\exp[-i\theta\sigma_z \otimes I_2 \otimes \sigma_z]$ |
| $\mathcal{B}^{(4)}_{1278}(\theta)$ | $\exp[-i\theta\sigma_z \otimes I_2 \otimes I_2 \otimes \sigma_z]$ | $\exp[-i\theta I_2 \otimes \sigma_z \otimes \sigma_z]$ |
| $\mathcal{B}^{(4)}_{3456}(\theta)$ | $\exp[-i\theta I_2 \otimes \sigma_z \otimes \sigma_z \otimes I_2]$ | $\exp[-i\theta I_2 \otimes \sigma_z \otimes \sigma_z]$ |
| $\mathcal{B}^{(4)}_{3478}(\theta)$ | $\exp[-i\theta\sigma_z \otimes I_2 \otimes \sigma_z \otimes I_2]$ | $\exp[-i\theta\sigma_z \otimes I_2 \otimes \sigma_z]$ |
| $\mathcal{B}^{(4)}_{5678}(\theta)$ | $\exp[-i\theta\sigma_z \otimes \sigma_z \otimes I_2 \otimes I_2]$ | $\exp[-i\theta\sigma_z \otimes \sigma_z \otimes I_2]$ |
| $\mathcal{B}^{(6)}_{123456}(\theta)$ | $\exp[-i\theta I_2 \otimes \sigma_z \otimes \sigma_z \otimes \sigma_z]$ | $\exp[-i\theta\sigma_z \otimes I_4]$ |
| $\mathcal{B}^{(6)}_{123478}(\theta)$ | $\exp[-i\theta\sigma_z \otimes I_2 \otimes \sigma_z \otimes \sigma_z]$ | $\exp[-i\theta I_2 \otimes \sigma_z \otimes I_2]$ |
| $\mathcal{B}^{(6)}_{125678}(\theta)$ | $\exp[-i\theta\sigma_z \otimes \sigma_z \otimes I_2 \otimes \sigma_z]$ | $\exp[-i\theta I_4 \otimes \sigma_z]$ |
| $\mathcal{B}^{(6)}_{345678}(\theta)$ | $\exp[-i\theta\sigma_z \otimes \sigma_z \otimes \sigma_z \otimes I_2]$ | $\exp[-i\theta\sigma_z \otimes \sigma_z \otimes \sigma_z]$ |
| $\mathcal{B}^{(8)}_{12345678}(\theta)$ | $\exp[-i\theta\sigma_z \otimes \sigma_z \otimes \sigma_z \otimes \sigma_z]$ | $\exp[-i\theta I_8]$ |

(B37)

It follows from Eq. (B37) that

$$\mathcal{B}_{12}(\theta) \approx \mathcal{B}_{345678}(\theta), \quad \mathcal{B}_{34}(\theta) \approx \mathcal{B}_{125678}(\theta),$$
$$\mathcal{B}_{56}(\theta) \approx \mathcal{B}_{123478}(\theta), \quad \mathcal{B}_{78}(\theta) \approx \mathcal{B}_{123456}(\theta),$$
$$\mathcal{B}_{1234}(\theta) \approx \mathcal{B}_{5678}(\theta), \quad \mathcal{B}_{1256}(\theta) \approx \mathcal{B}_{3478}(\theta),$$
$$\mathcal{B}_{1278}(\theta) \approx \mathcal{B}_{3456}(\theta), \tag{B38}$$

showing that the complementary operators $\mathcal{B}_\alpha(\theta)$ and $\mathcal{B}_{\overline{\alpha}}(\theta)$ give an identical logical quantum gate, where $\overline{\alpha}$ indicates the complementary set of $\alpha$. For instance, $\alpha = 56$ and $\overline{\alpha} = 123478$ in the case of $N = 4$.

#### 5. Three logical qubits

Three logical qubits are constructed from four physical qubits by taking the even-parity basis,

$$\mathcal{B}_{12} \simeq \mathrm{diag}(e^{-i\theta}, e^{i\theta}, e^{i\theta}, e^{-i\theta}, e^{i\theta}, e^{-i\theta}, e^{-i\theta}, e^{i\theta})$$
$$= \exp[-i\theta\sigma_z \otimes \sigma_z \otimes \sigma_z],$$
$$\mathcal{B}_{23} \simeq I_2 \otimes I_2 \otimes R_x(2\theta),$$
$$\mathcal{B}_{34} \simeq \exp[-i\theta I_2 \otimes I_2 \otimes \sigma_z] = I_2 \otimes I_2 \otimes R_z(2\theta),$$
$$\mathcal{B}_{45} \simeq I_2 \otimes U_{xx}(2\theta),$$
$$\mathcal{B}_{56} \simeq \exp[-i\theta I_2 \otimes \sigma_z \otimes I_2] = I_2 \otimes R_z(2\theta) \otimes I_2,$$
$$\mathcal{B}_{67} \simeq U_{xx}(2\theta) \otimes I_2,$$
$$\mathcal{B}_{78} \simeq \exp[-i\theta\sigma_z \otimes I_4] = R_z(2\theta) \otimes I_4. \tag{B39}$$

We find that controlled-controlled phase shift gate cannot be implemented only by diagonal braiding. It is proved by counting the number of the degrees of freedom. We need to tune seven parameters for the diagonal quantum gates. On the other hand, there are only three independent angle because the diagonal operators are $\mathcal{B}_1$, $\mathcal{B}_3$, and $\mathcal{B}_5$. Hence, it is impossible to construct controlled-controlled phase shift gate in general. However, this problem is solved by introducing many-body Majorana interaction,

$$U_{\mathrm{CC}\phi} \simeq \mathcal{B}_{12}\left(\frac{\phi}{8}\right)\mathcal{B}_{34}\left(\frac{\phi}{8}\right)\mathcal{B}_{56}\left(\frac{\phi}{8}\right)\mathcal{B}_{78}\left(\frac{\phi}{8}\right) \times \mathcal{B}^{(4)}_{1234}\left(-\frac{\phi}{8}\right)\mathcal{B}^{(4)}_{1278}\left(-\frac{\phi}{8}\right)\mathcal{B}^{(4)}_{1256}\left(-\frac{\phi}{8}\right). \tag{B40}$$

Especially, the CCZ gate is constructed as follows:

$$U_{\mathrm{CCZ}} \simeq \mathcal{B}_{12}\left(\frac{\pi}{8}\right)\mathcal{B}_{34}\left(\frac{\pi}{8}\right)\mathcal{B}_{56}\left(\frac{\pi}{8}\right)\mathcal{B}_{78}\left(\frac{\pi}{8}\right) \times \mathcal{B}^{(4)}_{1234}\left(-\frac{\pi}{8}\right)\mathcal{B}^{(4)}_{1278}\left(-\frac{\pi}{8}\right)\mathcal{B}^{(4)}_{1256}\left(-\frac{\pi}{8}\right). \tag{B41}$$

The Toffoli gate (i.e., CCNOT gate) is constructed by applying the Hadamard gate to the CCZ gate as in

$$U_{\mathrm{Toffloi}} = (I_4 \otimes U_H)U_{\mathrm{CCZ}}(I_4 \otimes U_H). \tag{B42}$$

See Fig. 2(a2) in the main text.

The Fredkin (i.e., CSWAP) gate is constructed by sequential applications of three Toffoli gates as in

$$U_{\mathrm{Fredkin}} = U^{(3,2)\to 1}_{\mathrm{Toffoli}} U^{(3,1)\to 2}_{\mathrm{Toffoli}} U^{(3,2)\to 1}_{\mathrm{Toffoli}}. \tag{B43}$$

See Fig. 2(b2) in the main text.

For example, the CZ gate in three qubits are embedded as

$$U^{3\to 2}_{\mathrm{CZ}} = U_{\mathrm{CZ}} \otimes I_2 = e^{i\pi/4}\mathcal{B}_{56}\left(\frac{\pi}{4}\right)\mathcal{B}_{78}\left(\frac{\pi}{4}\right)\mathcal{B}^{(4)}_{5678}\left(-\frac{\pi}{4}\right),$$
$$U^{3\to 1}_{\mathrm{CZ}} = e^{i\pi/4}\mathcal{B}_{34}\left(\frac{\pi}{4}\right)\mathcal{B}_{78}\left(\frac{\pi}{4}\right)\mathcal{B}^{(4)}_{3478}\left(-\frac{\pi}{4}\right),$$
$$U^{2\to 1}_{\mathrm{CZ}} = I_2 \otimes U_{\mathrm{CZ}} = e^{i\pi/4}\mathcal{B}_{34}\left(\frac{\pi}{4}\right)\mathcal{B}_{56}\left(\frac{\pi}{4}\right)\mathcal{B}^{(4)}_{3456}\left(-\frac{\pi}{4}\right), \tag{B44}$$

where $U^{p\to q}_{\mathrm{CZ}}$ indicates that the controlled qubit is $p$ and the target qubit is $q$. The CC$\phi$ phase-shift gate acting on three logical qubits in given by

$$U_{\mathrm{CC}\phi} = e^{i\phi/8}\mathcal{B}_{12}\left(\frac{\phi}{8}\right)\mathcal{B}_{34}\left(\frac{\phi}{8}\right)\mathcal{B}_{56}\left(\frac{\phi}{8}\right)\mathcal{B}_{78}\left(\frac{\phi}{8}\right) \times \mathcal{B}^{(4)}_{1234}\left(-\frac{\phi}{8}\right)\mathcal{B}^{(4)}_{1278}\left(-\frac{\phi}{8}\right)\mathcal{B}^{(4)}_{1256}\left(-\frac{\phi}{8}\right). \tag{B45}$$

Especially, the CCZ gate is constructed as follows:

$$U_{\mathrm{CCZ}} = e^{i\pi/8}\mathcal{B}_{12}\left(\frac{\pi}{8}\right)\mathcal{B}_{34}\left(\frac{\pi}{8}\right)\mathcal{B}_{56}\left(\frac{\pi}{8}\right)\mathcal{B}_{78}\left(\frac{\pi}{8}\right) \times \mathcal{B}^{(4)}_{1234}\left(-\frac{\pi}{8}\right)\mathcal{B}^{(4)}_{1256}\left(-\frac{\pi}{8}\right)\mathcal{B}^{(4)}_{1278}\left(-\frac{\pi}{8}\right). \tag{B46}$$

#### 6. Four logical qubits

We summarize results on constructing full set of Pauli Z gate for four logical qubits in the following table:

| Four logical qubits | |
|---|---|
| $\mathcal{B}_{12}(\theta)$ | $\exp[-i\theta\sigma_z \otimes \sigma_z \otimes \sigma_z \otimes \sigma_z]$ |
| $\mathcal{B}_{34}(\theta)$ | $\exp[-i\theta I_8 \otimes \sigma_z]$ |
| $\mathcal{B}_{56}(\theta)$ | $\exp[-i\theta I_4 \otimes \sigma_z \otimes I_2]$ |
| $\mathcal{B}_{78}(\theta)$ | $\exp[-i\theta I_2 \otimes \sigma_z \otimes I_4]$ |
| $\mathcal{B}_{9,10}(\theta)$ | $\exp[-i\theta\sigma_z \otimes I_8]$ |
| $\mathcal{B}^{(4)}_{1234}(\theta)$ | $\exp[-i\theta\sigma_z \otimes \sigma_z \otimes \sigma_z \otimes I_2]$ |
| $\mathcal{B}^{(4)}_{1256}(\theta)$ | $\exp[-i\theta\sigma_z \otimes \sigma_z \otimes I_2 \otimes \sigma_z]$ |
| $\mathcal{B}^{(4)}_{1278}(\theta)$ | $\exp[-i\theta\sigma_z \otimes I_2 \otimes \sigma_z \otimes \sigma_z]$, |
| $\mathcal{B}^{(4)}_{1290}(\theta)$ | $\exp[-i\theta I_2 \otimes \sigma_z \otimes \sigma_z \otimes \sigma_z]$ |
| $\mathcal{B}^{(4)}_{3456}(\theta)$ | $\exp[-i\theta I_2 \otimes I_2 \otimes \sigma_z \otimes \sigma_z]$ |
| $\mathcal{B}^{(4)}_{3478}(\theta)$ | $\exp[-i\theta I_2 \otimes \sigma_z \otimes I_2 \otimes \sigma_z]$ |
| $\mathcal{B}^{(4)}_{3490}(\theta)$ | $\exp[-i\theta\sigma_z \otimes I_4 \otimes \sigma_z]$ |
| $\mathcal{B}^{(4)}_{5678}(\theta)$ | $\exp[-i\theta I_2 \otimes \sigma_z \otimes \sigma_z \otimes I_2]$ |
| $\mathcal{B}^{(4)}_{5690}(\theta)$ | $\exp[-i\theta\sigma_z \otimes I_2 \otimes \sigma_z \otimes I_2]$ |
| $\mathcal{B}^{(4)}_{7890}(\theta)$ | $\exp[-i\theta\sigma_z \otimes \sigma_z \otimes I_4]$ |

(B47)

where 0 is an abbreviation of 10. The CZ gate is embedded as

$$U^{2\to 1}_{\mathrm{CZ}} = I_4 \otimes U_{\mathrm{CZ}} \simeq \mathcal{B}_{34}\left(\frac{\pi}{4}\right)\mathcal{B}_{56}\left(\frac{\pi}{4}\right)\mathcal{B}^{(4)}_{3456}\left(-\frac{\pi}{4}\right),$$
$$U^{3\to 2}_{\mathrm{CZ}} = I_2 \otimes U_{\mathrm{CZ}} \otimes I_2 \simeq \mathcal{B}_{56}\left(\frac{\pi}{4}\right)\mathcal{B}_{78}\left(\frac{\pi}{4}\right)\mathcal{B}^{(4)}_{5678}\left(-\frac{\pi}{4}\right),$$
$$U^{4\to 3}_{\mathrm{CZ}} = U_{\mathrm{CZ}} \otimes I_4 \simeq \mathcal{B}_{78}\left(\frac{\pi}{4}\right)\mathcal{B}_{9,10}\left(\frac{\pi}{4}\right)\mathcal{B}^{(4)}_{7890}\mathcal{B}^{(4)}_{7890},$$

$$U_{\mathrm{CZ}}^{3\to1}=\mathcal{B}_{34}\left(\frac{\pi}{4}\right)\mathcal{B}_{78}\left(\frac{\pi}{4}\right)\mathcal{B}_{3478}^{(4)}\left(-\frac{\pi}{4}\right),$$
$$U_{\mathrm{CZ}}^{4\to2}=\mathcal{B}_{56}\left(\frac{\pi}{4}\right)\mathcal{B}_{9,10}\left(\frac{\pi}{4}\right)\mathcal{B}_{5690}^{(4)}\left(-\frac{\pi}{4}\right). \quad \text{(B48)}$$

The CCC$\phi$ gate is explicitly constructed as

$$\begin{aligned}U_{\mathrm{C}^3\phi}=&\mathcal{B}_{34}\left(\frac{\phi}{16}\right)\mathcal{B}_{56}\left(\frac{\phi}{16}\right)\mathcal{B}_{78}\left(\frac{\phi}{16}\right)\mathcal{B}_{90}\left(\frac{\phi}{16}\right)\\&\times\mathcal{B}_{1234}^{(4)}\left(\frac{\phi}{16}\right)\mathcal{B}_{1256}^{(4)}\left(\frac{\phi}{16}\right)\mathcal{B}_{1278}^{(4)}\left(\frac{\phi}{16}\right)\\&\times\mathcal{B}_{1290}^{(4)}\left(\frac{\phi}{16}\right)\mathcal{B}_{3456}^{(4)}\left(-\frac{\phi}{16}\right)\mathcal{B}_{3478}^{(4)}\left(-\frac{\phi}{16}\right)\\&\times\mathcal{B}_{3490}^{(4)}\left(-\frac{\phi}{16}\right)\mathcal{B}_{5678}^{(4)}\left(\frac{\phi}{16}\right)\mathcal{B}_{5690}^{(4)}\left(-\frac{\phi}{16}\right)\\&\times\mathcal{B}_{7890}^{(4)}\left(-\frac{\phi}{16}\right)\mathcal{B}_{12}^{(4)}\left(-\frac{\phi}{16}\right).\end{aligned} \quad \text{(B49)}$$

### 7. $N+1$ physical qubits

We consider the $2N+2$ Majorana fermion system. The explicit actions of the adjacent braiding on $N+1$ physical qubits are given by

$$\begin{aligned}\mathcal{B}_{12}(\theta)&\simeq I_{2N}\otimes R_z(2\theta),\\\mathcal{B}_{34}(\theta)&\simeq I_{2N-2}\otimes R_z(2\theta)\otimes I_2,\\&\cdots\\\mathcal{B}_{2n-1,2n}(\theta)&\simeq I_{2N-2n+2}\otimes R_z(2\theta)\otimes I_{2n-2},\\&\cdots\\\mathcal{B}_{2N+1,2N+2}(\theta)&\simeq R_z(2\theta)\otimes I_{2N},\end{aligned} \quad \text{(B50)}$$

for odd numbers, and

$$\begin{aligned}\mathcal{B}_{23}(\theta)&\simeq I_{2N-2}\otimes U_{xx}(\theta),\\&\cdots\\\mathcal{B}_{2n,2n+1}(\theta)&\simeq I_{2N-2n}\otimes U_{xx}(\theta)\otimes I_{2n-2},\\&\cdots\\\mathcal{B}_{2N,2N+1}(\theta)&\simeq U_{xx}(\theta)\otimes I_{2N-2},\end{aligned} \quad \text{(B51)}$$

for even numbers, where

$$R_z(\theta)\equiv\exp\left[-i(\theta/2)\sigma_z\right]=\mathrm{diag}(e^{-i\theta/2},e^{i\theta/2}) \quad \text{(B52)}$$

is the rotation along the $z$ axis acting on one qubit and

$$U_{xx}(\theta)\equiv\exp\left[-i(\theta/2)\sigma_x\otimes\sigma_x\right] \quad \text{(B53)}$$

is the XX gate acting on two qubits.

## APPENDIX C: $N$ LOGICAL QUBITS

$N$ logical qubits are constructed from $N+1$ even physical qubits based on the correspondence,

$$\begin{pmatrix}\overbrace{\phantom{|0,\cdots,0,0,0\rangle}}^{N}\\|0,\cdots,0,0,0\rangle\\|0,\cdots,0,0,1\rangle\\|0,\cdots,0,1,0\rangle\\|0,\cdots,0,1,1\rangle\\|0,\cdots,1,0,0\rangle\\|0,\cdots,1,0,1\rangle\\\cdots\end{pmatrix}_{\text{logical}}\Leftrightarrow\begin{pmatrix}\overbrace{\phantom{|0,\cdots,0,0,0,0\rangle}}^{N+1}\\|0,\cdots,0,0,0,0\rangle\\|0,\cdots,0,0,1,1\rangle\\|0,\cdots,0,1,0,1\rangle\\|0,\cdots,0,1,1,0\rangle\\|0,\cdots,1,0,0,1\rangle\\|0,\cdots,1,0,1,0\rangle\\\cdots\end{pmatrix}_{\text{physical}}^{\text{even}}. \quad \text{(C1)}$$

The explicit actions of the braiding on even physical qubits corresponding to Eq. (B50) are

$$\begin{aligned}\mathcal{B}_{12}(\theta)&\simeq\exp\left[-i\theta\bigotimes_{j=1}^{N}\sigma_z\right],\\\mathcal{B}_{34}(\theta)&\simeq I_{2N-2}\otimes R_z(2\theta),\\&\cdots\\\mathcal{B}_{2n-1,2n}(\theta)&\simeq I_{2N-2n+2}\otimes R_z(2\theta)\otimes I_{2n-4}\\&=\exp\left[-i\theta I_{2N-2n+2}\otimes\sigma_z\otimes I_{2n-4}\right],\\&\cdots\\\mathcal{B}_{2N-3,2N-2}(\theta)&\simeq I_2\otimes R_z(2\theta)\otimes I_{2N-2n-4}\\&=\exp\left[-i\theta I_2\otimes\sigma_z\otimes I_{2N-2n-4}\right],\\\mathcal{B}_{2N+1,2N+2}(\theta)&\simeq R_z(2\theta)\otimes I_{2N-2n-2}\\&=\exp\left[-i\theta\sigma_z\otimes I_{2N-2n-2}\right],\end{aligned} \quad \text{(C2)}$$

for odd numbers, where the local $z$ rotation $R_z(2\theta)$ is made for an arbitrary qubit. Those corresponding to Eq. (B51) are

$$\begin{aligned}\mathcal{B}_{23}(\theta)&\simeq I_{2N-2}\otimes R_x(2\theta),\\\mathcal{B}_{45}(\theta)&\simeq I_{2N-4}\otimes U_{xx}(2\theta),\\\mathcal{B}_{67}(\theta)&\simeq I_{2N-6}\otimes U_{xx}(2\theta)\otimes I_2,\\&\cdots\\\mathcal{B}_{2n,2n+1}(\theta)&\simeq I_{2N-2-2n}\otimes U_{xx}(2\theta)\otimes I_{2n-2},\\&\cdots,\\\mathcal{B}_{2N,2N+1}(\theta)&\simeq U_{xx}(2\theta)\otimes I_{2N-4},\end{aligned} \quad \text{(C3)}$$

for even numbers, where only the local $x$ rotation $R_x(2\theta)$ acting on the first qubit is made by the braiding $\mathcal{B}_{23}(\theta)$, while $U_{xx}(2\theta)$ is given by Eq. (B23). On the other hand, by using $2N+2$-body interactions of Majorana fermions, the local $x$ rotation is made as in

$$\begin{aligned}\mathcal{B}_{23}(\theta)&\simeq I_{2N-2}\otimes R_x(2\theta),\\\mathcal{B}_{2}^{(4)}(\theta)&\simeq I_{2N-4}\otimes R_x(2\theta)\otimes I_2,\\\mathcal{B}_{2}^{(6)}(\theta)&\simeq I_{2N-6}\otimes R_x(2\theta)\otimes I_4,\\&\cdots\end{aligned}$$

$$\mathcal{B}_2^{(2N-2)}(\theta) \simeq I_2 \otimes R_x(2\theta) \otimes I_{2N-4},$$
$$\mathcal{B}_2^{(2N)}(\theta) \simeq R_x(2\theta) \otimes I_{2N-2}, \tag{C4}$$

with $B_\alpha^{(2N)}(\theta)$ defined by Eq. (16) in the main text, where

$$R_x(\theta) \equiv \exp\left[-i\frac{\theta}{2}\sigma_x\right] = \begin{pmatrix} \cos\frac{\theta}{2} & -i\sin\frac{\theta}{2} \\ -i\sin\frac{\theta}{2} & \cos\frac{\theta}{2} \end{pmatrix} \tag{C5}$$

is the rotation along the $x$ axis acting on one qubit.

Any one-qubit gate is given by

$$U_{1\text{bit}}(\theta,\phi) = e^{i(\phi+\pi)/2} R_z(\phi+\pi) U_H R_z(\theta) U_H$$
$$= \begin{pmatrix} \cos\frac{\theta}{2} & -i\sin\frac{\theta}{2} \\ ie^{i\phi}\sin\frac{\theta}{2} & -e^{i\phi}\cos\frac{\theta}{2} \end{pmatrix}. \tag{C6}$$

The $C^s$-phase shift gate is a diagonal operator. Using the relation

$$U_{C^s\phi} = e^{\frac{i\phi}{2^{s+1}}} \prod_{q=1}^{2^{s+1}-1} \exp\left[\frac{(-1)^{\text{Mod}_2 \sum_{p=1}^{s+1} p_s}}{2^{s+1}} \bigotimes_{p=1}^{s+1} (\sigma_z)^{q_p}\right] \tag{C7}$$

with $q_p = 0, 1$, it is constructed as

$$U_{C^s\phi} = e^{\frac{i\phi}{2^{s+1}}} \prod_{q=1}^{2^n} \mathcal{B}_{\text{odd},q}\left(\frac{\phi}{2^{s+1}}\right) \prod_{r=1}^{2^s-1} \mathcal{B}_{\text{even},r}\left(-\frac{\phi}{2^{s+1}}\right), \tag{C8}$$

where $B_{\text{odd}}$ contains odd number of $\sigma_z$ operators for logical qubits, while $\mathcal{B}_{\text{even}}$ contains even number of $\sigma_z$ operators for logical qubits. By setting $\phi = \pi$, we obtain the $C^r Z$ gate.

For example,

$$U_{C\phi} \equiv \{1, 1, 1, e^{i\phi}\} = e^{i\phi/4} e^{-\frac{i\phi}{4} I_2\otimes\sigma_z} e^{-\frac{i\phi}{4}\sigma_z\otimes I_2} e^{\frac{i\phi}{4}\sigma_z\otimes\sigma_z},$$
$$U_{CC\phi} \equiv \{1, 1, 1, 1, 1, 1, 1, e^{i\phi}\}$$
$$= e^{i\phi/8} e^{-\frac{i\phi}{8} I_2\otimes I_2\otimes\sigma_z} e^{-\frac{i\phi}{8} I_2\otimes\sigma_z\otimes I_2} e^{-\frac{i\phi}{8}\sigma_z\otimes\sigma_z\otimes I_2} e^{\frac{i\phi}{8} I_2\otimes\sigma_z\otimes\sigma_z} e^{\frac{i\phi}{8}\sigma_z\otimes I_2\otimes\sigma_z} e^{\frac{i\phi}{8}\sigma_z\otimes\sigma_z\otimes I_2} e^{-\frac{i\phi}{8}\sigma_z\otimes\sigma_z\otimes\sigma_z},$$
$$U_{CCC\phi} \equiv \{1, 1, 1, 1, 1, 1, 1, 1, 1, 1, 1, 1, 1, 1, 1, e^{i\phi}\}$$
$$= e^{i\phi/16} e^{-\frac{i\phi}{16} I_2\otimes I_2\otimes I_2\otimes\sigma_z} e^{-\frac{i\phi}{16} I_2\otimes I_2\otimes\sigma_z\otimes I_2} e^{-\frac{i\phi}{16} I_2\otimes\sigma_z\otimes I_2\otimes I_2} e^{-\frac{i\phi}{16}\sigma_z\otimes I_2\otimes I_2\otimes I_2}$$
$$\times e^{\frac{i\phi}{16} I_2\otimes I_2\otimes\sigma_z\otimes\sigma_z} e^{\frac{i\phi}{16} I_2\otimes\sigma_z\otimes I_2\otimes\sigma_z} e^{\frac{i\phi}{16}\sigma_z\otimes I_2\otimes I_2\otimes\sigma_z} e^{\frac{i\phi}{16} I_2\otimes\sigma_z\otimes\sigma_z\otimes I_2} e^{\frac{i\phi}{16}\sigma_z\otimes I_2\otimes\sigma_z\otimes I_2} e^{\frac{i\phi}{16}\sigma_z\otimes\sigma_z\otimes I_2\otimes I_2}$$
$$\times e^{-\frac{i\phi}{16} I_2\otimes\sigma_z\otimes\sigma_z\otimes\sigma_z} e^{-\frac{i\phi}{16}\sigma_z\otimes I_2\otimes\sigma_z\otimes\sigma_z} e^{-\frac{i\phi}{16}\sigma_z\otimes\sigma_z I_2\otimes\otimes\sigma_z} e^{-\frac{i\phi}{16}\sigma_z\otimes\sigma_z\otimes\sigma_z\otimes I_2} e^{\frac{i\phi}{16}\sigma_z\otimes\sigma_z\otimes\sigma_z\otimes\sigma_z}. \tag{C9}$$

The Toffoli (CCNOT) gate is constructed by applying the Hadamard gate to the CCZ gate as in

$$U_{\text{Toffloi}} = (I_4 \otimes U_H) U_{CCZ} (I_4 \otimes U_H). \tag{C10}$$

See Fig. 8(a1). The Fredkin (CSWAP) gate is constructed by sequential applications of three Toffoli gates as in

$$U_{\text{Fredkin}} = U_{\text{Toffoli}}^{(3,2)\to 1} U_{\text{Toffoli}}^{(3,1)\to 2} U_{\text{Toffoli}}^{(3,2)\to 1}, \tag{C11}$$

where $U_{CZ}^{(p,q)\to r}$ indicates that the controlled qubits are $p$ and $q$ while the target qubit is $r$. See Fig. 8(b1).

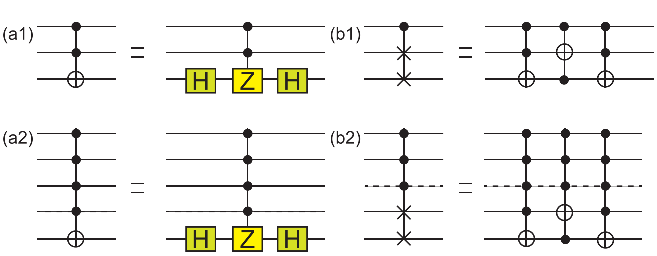


FIG. 8. (a1) Construction of the CCNOT gate from the CCZ gate and the Hadamard gates. (a2) Construction of the $C^n$NOT gate from the $C^n$Z gate and the Hadamard gates. (b1) Construction of the Fredkin gate from three Toffoli gates. (b2) Construction of the $C^n$SWAP gate from the $C^n$NOT gates.

The $C^n$NOT gate is constructed from $C^n$Z gate as

$$U_{C^n\text{NOT}} = (I_{2n-2} \otimes U_H) U_{C^n Z} (I_{2n-2} \otimes U_H), \tag{C12}$$

where the Hadamard gate is applied to $n$th qubit. See Fig. 8(a2).

The $C^n$SWAP gate is constructed from the $C^n$Z gate as

$$U_{C^n\text{SWAP}} = U_{C^n\text{NOT}}^{\bar{1}\to 1} U_{C^n\text{NOT}}^{\bar{2}\to 2} U_{C^n\text{NOT}}^{\bar{1}\to 1}, \tag{C13}$$

where $U_{C^n\text{NOT}}^{\bar{p}\to p}$ indicates that the target qubit is $p$ and the others are controlled qubits, where $\bar{p}$ indicates the complementary qubits of the qubit $p$. See Fig. 8(b2).

### Diagonal gates

We construct an arbitrary diagonal gate in terms of braiding and many-body interactions. We show that it is possible to construct any $2^{N+1}$ diagonal operators based on $2(N+1)$-body Majorana interactions. There are ${}_{N+1}C_M$ patterns of $2M$-body unitary evolutions in $2(N+1)$ physical qubits. By taking a sum, we have $\sum_{M=1}^{N+1} {}_{N+1}C_M = 2^{N+1}$ independent physical qubits. They produce $2^N$ independent logical qubits because there are complementary operators $\mathcal{B}_\alpha(\theta)$ and $\mathcal{B}_{\overline{\alpha}}(\theta)$ which produce the same logical qubits. See Appendix B4 with respect to the complementary operators. On the other hand, there are $2^N$ independent many-body Majorana operators. Hence, it is possible to construct arbitrary diagonal operators by solving appropriate linear equations.

### APPENDIX D: EXPERIMENTAL REALIZATION

The two-body operation is realized by the unitary dynamics during $0 \leqslant t \leqslant T$,

$$\mathcal{B}_{\alpha\beta}(\theta) = \exp[\theta\gamma_\beta\gamma_\alpha] = \exp[iHt/\hbar], \tag{D1}$$

with $H = (\hbar\theta/iT)\gamma_\beta\gamma_\alpha$. A $2N$-body Majorana operation is realized by a dynamics driven by $2N$-body interaction of Majorana fermions during $0 \leqslant t \leqslant T$,

$$\mathcal{B}^{(2N)}_{\alpha}(\theta) = \exp[iHt/\hbar], \tag{D2}$$

with $H = (i^{N-2}\hbar\theta/T)\gamma_{2N}\gamma_{2N-1}\cdots\gamma_2\gamma_1$.

#### 1. Topological superconductor realization

In topological superconductors, Majorana fermions are constructed from fermion operators,

$$c_\alpha = (\gamma_{2\alpha-1} + i\gamma_{2\alpha})/2. \tag{D3}$$

The fermion density operator is rewritten in terms of Majorana operators as

$$\rho_\alpha = c^\dagger_\alpha c_\alpha = (1 + i\gamma_{2\alpha-1}\gamma_{2\alpha})/2, \tag{D4}$$

or $i\gamma_{2\alpha-1}\gamma_{2\alpha} = 2\rho_\alpha - 1$. The four-body interaction necessary in universal computation is represented in terms of the density operator as $\gamma_{2\alpha-1}\gamma_{2\alpha}\gamma_{2b-1}\gamma_{2\beta} = -(2\rho_\alpha - 1)(2\rho_\beta - 1)$. It is realized by the Coulomb interaction.

In the similar way, $2N$-body interaction is represented in terms of the $N$-body density operator

$$\begin{aligned}&\gamma_{2\alpha_1-1}\gamma_{2\alpha_1}\gamma_{2\alpha_2-1}\gamma_{2\alpha_2}\cdots\gamma_{2\alpha_N-1}\gamma_{2\alpha_N}\\ &\quad= i^N(2\rho_{\alpha_1}-1)(2\rho_{\alpha_2}-1)\cdots(2\rho_{\alpha_N}-1),\end{aligned} \tag{D5}$$

which is realized by a many-body interaction [51] and derived as an effective interaction by integrating out the high-energy excitations. Hence, the many-body Majorana interactions necessary for universal quantum computation are experimentally feasible.

#### 2. Spin system realization

In the Kitaev spin liquid model [28], Majorana fermion operators are constructed from spin operators. It is realized in qubits [62,63], trapped ions [64], cold atoms [65,66], and quantum dots [67]. Spin operators are transformed into Majorana fermion operators by using the Jordan-Wigner transformation [68–74] defined by $\sigma^-_i = \Omega_i c_i$, $\sigma^+_i = \Omega_i c^\dagger_i$, $\sigma^z_i = c^\dagger_i c_i - \frac{1}{2}$, where $c_i$ ($c^\dagger_i$) is the fermion annihilation (creation) operators, $\Omega_i =^{i-1}_{j=1} \exp[i\pi c^\dagger_i c_i]$, $\sigma^+ = \frac{1}{2}(\sigma^x + i\sigma^y)$, and $\sigma^- = \frac{1}{2}(\sigma^x - i\sigma^y)$. We introduce Majorana fermion operators,

$$\begin{aligned}\gamma^A_{2j} &= c_{2j} + c^\dagger_{2j}, \quad \gamma^B_{2j} = -i(c_{2j} - c^\dagger_{2j}),\\ \gamma^A_{2j+1} &= -i(c_{2j+1} - c^\dagger_{2j+1}), \quad \gamma^B_{2j+1} = c_{2j+1} + c^\dagger_{2j+1}.\end{aligned} \tag{D6}$$

The spin operators are rewritten in terms of Majorana fermion operators as

$$\begin{aligned}\sigma^x_{2j-1}\sigma^x_{2j} &= i\gamma^A_{2j-1}\gamma^A_{2j}, \quad \sigma^y_{2j}\sigma^y_{2j+1} = -i\gamma^A_{2j}\gamma^A_{2j+1},\\ \sigma^z_{2j-1} &= -i\gamma^A_{2j-1}\gamma^B_{2j-1}, \quad \sigma^z_{2j} = i\gamma^A_{2j}\gamma^B_{2j}.\end{aligned} \tag{D7}$$

The Ising interaction gives the four-body Majorana interaction

$$\sigma^z_{2j-1}\sigma^z_{2j} = \gamma^A_{2j-1}\gamma^B_{2j-1}\gamma^A_{2j}\gamma^B_{2j}. \tag{D8}$$

The three-body interaction of spins in the form of $\sigma^z_1\sigma^z_2\sigma^z_3$ is experimentally realized in a superconducting qubit system [75,76], which gives the six-body Majorana interaction

$$\sigma^z_{\alpha_1}\sigma^z_{\alpha_2}\sigma^z_{\alpha_3} \propto \gamma^A_{\alpha_1}\gamma^B_{\alpha_1}\gamma^A_{\alpha_2}\gamma^B_{\alpha_2}\gamma^A_{\alpha_3}\gamma^B_{\alpha_3}. \tag{D9}$$

The $N$-body Ising interaction is realized in qubit systems [77], which gives $2N$-body Majorana interactions

$$\sigma^z_{\alpha_1}\sigma^z_{\alpha_2}\cdots\sigma^z_{\alpha_N} \propto \gamma^A_{\alpha_1}\gamma^B_{\alpha_1}\gamma^A_{\alpha_2}\gamma^B_{\alpha_2}\cdots\gamma^A_{\alpha_N}\gamma^B_{\alpha_N}. \tag{D10}$$

Hence, the many-body Majorana interactions necessary for universal quantum computation are experimentally feasible.

### APPENDIX E: SPARCE ENCODING

We use $2N + 2$ Majorana fermions to construct $N$ logical qubits in the dense encoding discussed in the main text. On the other hand, it is necessary to use $4N$ Majorana fermions to construct $N$ logical qubits in the sparce encoding, where there is a correspondence,

$$\begin{pmatrix}|0\rangle\\|1\rangle\end{pmatrix}_{\text{logical}} = \begin{pmatrix}|0,0\rangle\\|1,1\rangle\end{pmatrix}_{\text{physical}} \tag{E1}$$

for each qubit.

Universal quantum computation is not possible only by braiding but is possible by adding many-body interactions as in the case of the dense encoding. Especially, $2N$-body interactions are necessary for $N$-qubit universal quantum computation as shown in the following.

#### 1. One logical qubit

We use four Majorana fermions for one logical qubit. The correspondence between the physical and logical qubits are

$$\begin{pmatrix}|0\rangle\\|1\rangle\end{pmatrix}_{\text{logical}} = \begin{pmatrix}|0,0\rangle\\|1,1\rangle\end{pmatrix}_{\text{physical}}. \tag{E2}$$

It is the same as the dense encoding. Hence, one qubit gate for the sparce encoding is identical to that for the dense cording.

#### 2. Two logical qubits

We use eight Majorana fermions for two logical qubits. The correspondence between the physical and logical qubits are

$$\begin{pmatrix}|0,0\rangle\\|0,1\rangle\\|1,0\rangle\\|1,1\rangle\end{pmatrix}_{\text{logical}} \Leftrightarrow \begin{pmatrix}|0,0,0,0\rangle\\|0,0,1,1\rangle\\|1,1,0,0\rangle\\|1,1,1,1\rangle\end{pmatrix}_{\text{physical}}. \tag{E3}$$

Logical quantum gates made by the braiding operators are

$$\begin{aligned}&\mathcal{B}_{12}(\theta) = \mathcal{B}_{34}(\theta) = \mathcal{B}^{(4)}_{125678}(\theta) = \mathcal{B}^{(4)}_{345678}(\theta) \simeq I_2 \otimes R_z(2\theta),\\ &\mathcal{B}_{23}(\theta) \simeq I_2 \otimes R_x(2\theta),\\ &\mathcal{B}_{45}(\theta) \simeq I_4 \cos\theta,\\ &\mathcal{B}_{56}(\theta) = \mathcal{B}_{78}(\theta) = \mathcal{B}^{(4)}_{123456}(\theta) = \mathcal{B}^{(4)}_{123478}(\theta) \simeq R_z(2\theta) \otimes I_2,\\ &\mathcal{B}_{67}(\theta) \simeq R_x(2\theta) \otimes I_2.\end{aligned} \tag{E4}$$

We note that different braiding operators give the same quantum gate such as $\mathcal{B}_{12}(\theta)$ and $\mathcal{B}_{34}(\theta)$. They are not sufficient for universal quantum computation.

In addition, four-body Majorana operators realize logical quantum gate,

$$\mathcal{B}^{(4)}_{1234}(\theta) = \mathcal{B}^{(4)}_{5678}(\theta) = \mathcal{B}^{(4)}_{12345678}(\theta) \simeq e^{-i\theta} I_4,$$
$$\mathcal{B}^{(4)}_{1256}(\theta) = \mathcal{B}^{(4)}_{1278}(\theta) = \mathcal{B}^{(4)}_{3456}(\theta) = \mathcal{B}^{(4)}_{3478}(\theta) \simeq \exp[-i\theta\sigma_z \otimes \sigma_z]. \quad \text{(E5)}$$

Hence, two-qubit universal quantum computation is possible by introducing four-body Majorana operators.

### 3. Three logical qubits

We use 12 Majorana fermions for three logical qubits. The correspondence between the physical and logical qubits are

$$\begin{pmatrix} |0,0,0\rangle \\ |0,0,1\rangle \\ |0,1,0\rangle \\ |0,1,1\rangle \\ |1,0,0\rangle \\ |1,0,1\rangle \\ |1,1,0\rangle \\ |1,1,1\rangle \end{pmatrix}_{\text{logical}} \Leftrightarrow \begin{pmatrix} |0,0,0,0,0,0\rangle \\ |0,0,0,0,1,1\rangle \\ |0,0,1,1,0,0\rangle \\ |0,0,1,1,1,1\rangle \\ |1,1,0,0,0,0\rangle \\ |1,1,0,0,1,1\rangle \\ |1,1,1,1,0,0\rangle \\ |1,1,1,1,1,1\rangle \end{pmatrix}_{\text{physical}}. \quad \text{(E6)}$$

Quantum gates made by the braiding operators are

$$\begin{aligned}
\mathcal{B}_{12}(\theta) &= \mathcal{B}_{34}(\theta) \simeq \exp[-i\theta I_4 \otimes \sigma_z] = I_4 \otimes R_z(2\theta), \\
\mathcal{B}_{23}(\theta) &\simeq I_4 \otimes R_x(2\theta), \\
\mathcal{B}_{56}(\theta) &= \mathcal{B}_{78}(\theta) \simeq \exp[-i\theta I_2 \otimes \sigma_z \otimes I_2] \\
&= I_2 \otimes R_z(2\theta) \otimes I_2, \\
\mathcal{B}_{9,10}(\theta) &= \mathcal{B}_{11,12}(\theta) \simeq \exp[-i\theta\sigma_z \otimes I_4] = R_z(2\theta) \otimes I_4, \\
\mathcal{B}_{45}(\theta) &= \mathcal{B}_{89}(\theta) \simeq I_8 \cos\theta, \\
\mathcal{B}_{67}(\theta) &\simeq I_2 \otimes R_x(2\theta) \otimes I_2, \\
\mathcal{B}_{10,11}(\theta) &\simeq R_x(2\theta) \otimes I_4.
\end{aligned} \quad \text{(E7)}$$

We note that different braiding operators give the same quantum gate such as $\mathcal{B}_{12}(\theta)$ and $\mathcal{B}_{34}(\theta)$. They are not sufficient for universal quantum computation.

In addition, four-body Majorana operators realize logical quantum gates,

$$\begin{aligned}
\mathcal{B}_{1234}(\theta) &= \mathcal{B}_{5678}(\theta) = \mathcal{B}_{9,10,11,12}(\theta) \simeq e^{-i\theta} I_8, \\
\mathcal{B}_{1256}(\theta) &= \mathcal{B}_{1278}(\theta) = \mathcal{B}_{3456}(\theta) = \mathcal{B}_{3478}(\theta) \\
&\simeq \exp[-i\theta I_2 \otimes \sigma_z \otimes \sigma_z], \\
\mathcal{B}_{129,10}(\theta) &= \mathcal{B}_{12,11,12}(\theta) = \mathcal{B}_{349,10}(\theta) = \mathcal{B}_{34,11,12}(\theta) \\
&\simeq \exp[-i\theta\sigma_z \otimes I_2 \otimes \sigma_z], \\
\mathcal{B}_{5678}(\theta) &= \mathcal{B}_{569,10}(\theta) = \mathcal{B}_{56,11,12}(\theta) = \mathcal{B}_{789,10}(\theta) \\
&= \mathcal{B}_{78,11,12}(\theta) \simeq \exp[-i\theta\sigma_z \otimes \sigma_z \otimes I_2],
\end{aligned} \quad \text{(E8)}$$

and six-body Majorana operators realize a logical quantum gate,

$$\mathcal{B}_{34569,10}(\theta) = \mathcal{B}_{3456,11,12}(\theta) \simeq \exp[-i\theta\sigma_z \otimes \sigma_z \otimes \sigma_z]. \quad \text{(E9)}$$

Hence, three-qubit universal quantum computation is possible by introducing four-body and six-body Majorana operators.

## APPENDIX F: GENERALIZED BRAID GROUP RELATION

We consider the case $\theta = \pi/4$. The Artin braid group relation reads [78],

$$\mathcal{B}_\alpha \mathcal{B}_\beta = \mathcal{B}_\beta \mathcal{B}_\alpha \quad \text{for} \quad |\alpha - \beta| \geqslant 2,$$
$$\mathcal{B}_\alpha \mathcal{B}_{\alpha+1} \mathcal{B}_\alpha = \mathcal{B}_{\alpha+1} \mathcal{B}_\alpha \mathcal{B}_{\alpha+1}. \quad \text{(F1)}$$

It is identical to the extraspecial 2 group [79]

$$M_\alpha^2 = -1, \quad M_\alpha M_{\alpha+1} = -M_{\alpha+1} M_\alpha,$$
$$M_a M_\beta = M_\beta M_\alpha, \quad \text{for} \quad |\alpha - \beta| \geqslant 2, \quad \text{(F2)}$$

by setting

$$\mathcal{B}^{(4)}_\alpha = \frac{1}{\sqrt{2}}(1 + M_\alpha). \quad \text{(F3)}$$

It is straightforward to show that

$$\begin{aligned}
\left(M^{(4)}_\alpha\right)^2 &= -1, \\
M^{(4)}_\alpha M^{(4)}_{\alpha+1} &= -M^{(4)}_{\alpha+1} M^{(4)}_\alpha, \\
M^{(4)}_\alpha M^{(4)}_{\alpha+2} &= M^{(4)}_{\alpha+2} M^{(4)}_\alpha, \\
M^{(4)}_\alpha M^{(4)}_{\alpha+3} &= -M^{(4)}_{\alpha+3} M^{(4)}_\alpha, \\
M^{(4)}_a M^{(4)}_\beta &= M^{(4)}_\beta M^{(4)}_\alpha \quad \text{for} \quad |\alpha - \beta| \geqslant 4,
\end{aligned} \quad \text{(F4)}$$

when we set

$$M^{(4)}_\alpha \equiv i\gamma_4\gamma_3\gamma_2\gamma_1. \quad \text{(F5)}$$

It is a generalization of the extraspecial 2 group. Correspondingly, we obtain a generalized braiding group relation,

$$\mathcal{B}^{(4)}_\alpha \mathcal{B}^{(4)}_{\alpha+1} \mathcal{B}^{(4)}_\alpha = \mathcal{B}^{(4)}_{\alpha+1} \mathcal{B}^{(4)}_\alpha \mathcal{B}^{(4)}_{\alpha+1},$$
$$\mathcal{B}^{(4)}_\alpha \mathcal{B}^{(4)}_{\alpha+3} \mathcal{B}^{(4)}_\alpha = \mathcal{B}^{(4)}_{\alpha+3} \mathcal{B}^{(4)}_\alpha \mathcal{B}^{(4)}_{\alpha+3}, \quad \text{(F6)}$$

and

$$\mathcal{B}^{(4)}_\alpha \mathcal{B}^{(4)}_\beta = \mathcal{B}^{(4)}_\beta \mathcal{B}^{(4)}_\alpha \quad \text{(F7)}$$

for $|\alpha - \beta| = 2$ and $|\alpha - \beta| \geqslant 4$. In the similar way, we find

$$\left(M^{(2N)}_\alpha\right)^2 = -1, \quad M^{(4)}_\alpha M^{(4)}_{\alpha+2n-1} = -M^{(4)}_{\alpha+2n-1} M^{(4)}_\alpha,$$
$$M^{(4)}_\alpha M^{(4)}_{\alpha+2n} = M^{(4)}_{\alpha+2n} M^{(4)}_\alpha,$$
$$M^{(4)}_a M^{(4)}_\beta = M^{(4)}_\beta M^{(4)}_\alpha \quad \text{for} \quad |\alpha - \beta| \geqslant 2N, \quad \text{(F8)}$$

for $1 \leqslant n \leqslant N$. Hence, the $2N$-body Majorana operators satisfy a generalized braiding group relation,

$$\mathcal{B}^{(2N)}_\alpha \mathcal{B}^{(2N)}_{\alpha+2n-1} \mathcal{B}^{(2N)}_\alpha = \mathcal{B}^{(2N)}_{\alpha+2n-1} \mathcal{B}^{(2N)}_\alpha \mathcal{B}^{(2N)}_{\alpha+2n-1}, \quad \text{(F9)}$$

and

$$\mathcal{B}^{(2N)}_\alpha \mathcal{B}^{(2N)}_\beta = \mathcal{B}^{(2N)}_\beta \mathcal{B}^{(2N)}_\alpha \quad \text{(F10)}$$

for $|\alpha - \beta| = 2n$, $|\alpha - \beta| \geqslant 2N$, and for $1 \leqslant n \leqslant N$.

[1] R. Feynman, Simulating physics with computers, Int. J. Theor. Phys. **21**, 467 (1982).
[2] D. P. DiVincenzo, Quantum computation, Science **270**, 255 (1995).
[3] M. Nielsen and I. Chuang, *Quantum Computation and Quantum Information* (Cambridge University Press, Cambridge, UK, 2016).
[4] D. Deutsch, Quantum theory, the church-turing principle and the universal quantum computer, Proc. Roy. Soc. A **400**, 97 (1985).
[5] C. M. Dawson and M. A. Nielsen, The Solovay-Kitaev algorithm, Quantum Inf. Comput. **6**, 81 (2006).
[6] M. Nielsen and I. Chuang, *Quantum Computation and Quantum Information* (Cambridge University Press, Cambridge, UK, 2010).
[7] Y. Nakamura, Yu. A. Pashkin, and J. S. Tsai, Coherent control of macroscopic quantum states in a single-Cooper-pair box, Nature (London) **398**, 786 (1999).
[8] E. Knill, R. Laflamme, and G. J. Milburn, A scheme for efficient quantum computation with linear optics, Nature (London) **409**, 46 (2001).
[9] D. Loss and D. P. DiVincenzo, Quantum computation with quantum dots, Phys. Rev. A **57**, 120 (1998).
[10] J. I. Cirac and P. Zoller, Quantum computations with cold trapped ions, Phys. Rev. Lett. **74**, 4091 (1995).
[11] L. M. K. Vandersypen, M. Steffen, G. Breyta, C. S. Yannoni, M. H. Sherwood, and I. L. Chuang, Experimental realization of Shor's quantum factoring algorithm using nuclear magnetic resonance, Nature (London) **414**, 883 (2001).
[12] B. E. Kane, A silicon-based nuclear spin quantum computer, Nature (London) **393**, 133 (1998).
[13] S. B. Bravyi and A. Yu. Kitaev, Fermionic quantum computation, Ann. Phys. **298**, 210 (2002).
[14] D. A. Ivanov, Non-Abelian statistics of half-quantum vortices in *p*-wave superconductors, Phys. Rev. Lett. **86**, 268 (2001).
[15] A. Kitaev, Fault-tolerant quantum computation by anyons, Ann. Phys. **303**, 2 (2003).
[16] S. D. Sarma, M. Freedman, and C. Nayak, Topologically protected qubits from a possible non-Abelian fractional quantum Hall state, Phys. Rev. Lett. **94**, 166802 (2005).
[17] C. Nayak, S. H. Simon, A. Stern, M. Freedman, and S. D. Sarma, Non-Abelian anyons and topological quantum computation, Rev. Mod. Phys. **80**, 1083 (2008).
[18] N. Read and D. Green, Paired states of fermions in two dimensions with breaking of parity and time-reversal symmetries and the fractional quantum Hall effect, Phys. Rev. B **61**, 10267 (2000).
[19] N. Read, Non-Abelian braid statistics versus projective permutation statistics, J. Math. Phys. **44**, 558 (2003).
[20] M. Freedman, C. Nayak, and K. Walker, Towards universal topological quantum computation in the $\nu = 5/2$ fractional quantum Hall state, Phys. Rev. B **73**, 245307 (2006).
[21] X.-L. Qi and S.-C. Zhang, Topological insulators and superconductors, Rev. Mod. Phys. **83**, 1057 (2011).
[22] M. Sato and Y. Ando, Topological superconductors: A review, Rep. Prog. Phys. **80**, 076501 (2017).
[23] S. R. Elliott and M. Franz, Majorana fermions in nuclear, particle, and solid-state physics, Rev. Mod. Phys. **87**, 137 (2015).
[24] S. D. Sarma, M. Freedman, and C. Nayak, Majorana zero modes and topological quantum computation, npj Quantum Inf. **1**, 15001 (2015).
[25] J. Alicea, Y. Oreg, G. Refael, F. von Oppen, and M. P. A. Fisher, Non-Abelian statistics and topological quantum information processing in 1D wire networks, Nat. Phys. **7**, 412 (2011).
[26] J. Alicea, New directions in the pursuit of Majorana fermions in solid state systems, Rep. Prog. Phys. **75**, 076501 (2012).
[27] C. W. J. Beenakker, Search for Majorana fermions in superconductors, Annu. Rev. Condens. Matter Phys. **4**, 113 (2013).
[28] A. Kitaev, Anyons in an exactly solved model and beyond, Ann. Phys. **321**, 2 (2006).
[29] Y. Kasahara, T. Ohnishi, Y. Mizukami, O. Tanaka, Sixiao Ma, K. Sugii, N. Kurita, H. Tanaka, J. Nasu, Y. Motome, T. Shibauchi, and Y. Matsuda, Majorana quantization and half-integer thermal quantum Hall effect in a Kitaev spin liquid, Nature (London) **559**, 227 (2018).
[30] S. Bravyi and A. Kitaev, Universal quantum computation with ideal Clifford gates and noisy ancillas, Phys. Rev. A **71**, 022316 (2005).
[31] A. Ahlbrecht, L. S. Georgiev, and R. F. Werner, Implementation of Clifford gates in the Ising-anyon topological quantum computer, Phys. Rev. A **79**, 032311 (2009).
[32] D. Gottesman, Stabilizer codes and quantum error correction, arXiv:quant-ph/9705052.
[33] D. Gottesman, The Heisenberg representation of quantum computers, arXiv:quant-ph/9807006.
[34] S. Aaronson and D. Gottesman, Improved simulation of stabilizer circuits, Phys. Rev. A **70**, 052328 (2004).
[35] S. Bravyi, Universal quantum computation with the $\nu = 5/2$ fractional quantum Hall state, Phys. Rev. A **73**, 042313 (2006).
[36] J. D. Sau, S. Tewari, and S. D. Sarma, Universal quantum computation in a semiconductor quantum wire network, Phys. Rev. A **82**, 052322 (2010).
[37] M. Leijnse and K. Flensberg, Quantum information transfer between topological and spin qubit systems, Phys. Rev. Lett. **107**, 210502 (2011).
[38] T. Hyart, B. van Heck, I. C. Fulga, M. Burrello, A. R. Akhmerov, and C. W. J. Beenakker, Flux-controlled quantum computation with Majorana fermions, Phys. Rev. B **88**, 035121 (2013).
[39] S. Hoffman, C. Schrade, J. Klinovaja, and D. Loss, Universal quantum computation with hybrid spin-Majorana qubits, Phys. Rev. B **94**, 045316 (2016).
[40] T. E. O'Brien, P. Rożek, and A. R. Akhmerov, Majorana-based fermionic quantum computation, Phys. Rev. Lett. **120**, 220504 (2018).
[41] P. Bonderson, S. D. Sarma, M. Freedman, and C. Nayak, A blueprint for a topologically fault-tolerant quantum computer, arXiv:1003.2856.
[42] P. Bonderson, L. Fidkowski, M. Freedman, and K. Walker, Twisted interferometry, arXiv:1306.2379.
[43] M. Barkeshli and J. D. Sau, Physical architecture for a universal topological quantum computer based on a network of Majorana nanowires, arXiv:1509.07135.
[44] T. Karzig, Y. Oreg, G. Refael, and M. H. Freedman, Phys. Rev. X **6**, 031019 (2016).
[45] L. S. Georgiev, Topologically protected gates for quantum computation with non-Abelian anyons in the Pfaffian quantum Hall state, Phys. Rev. B **74**, 235112 (2006).

[46] L. S. Georgiev, Towards a universal set of topologically protected gates for quantum computation with Pfaffian qubits, Nucl. Phys. B **789**, 552 (2008).

[47] C. Nayak and F. Wilczek, $2n$-quasihole states realize $2^{n-1}$-dimensional spinor braiding statistics in paired quantum Hall states, Nucl. Phys. B **479**, 529 (1996).

[48] L. S. Georgiev, Computational equivalence of the two inequivalent spinor representations of the braid group in the Ising topological quantum computer, J. Stat. Mech. (2009) P12013.

[49] L. S. Georgiev, Ultimate braid-group generators for coordinate exchanges of Ising anyons from the multi-anyon Pfaffian wavefunctions, J. Phys. A: Math. Theor. **42**, 225203 (2009).

[50] C. V. Kraus, P. Zoller, and M. A. Baranov, Braiding of atomic Majorana fermions in wire networks and implementation of the Deutsch-Jozsa algorithm, Phys. Rev. Lett. **111**, 203001 (2013).

[51] H. P. Büchler, A. Micheli, and P. Zoller, Three-body interactions with cold polar molecules, Nat. Phys. **3**, 726 (2007).

[52] H.-L. Huang *et al.*, Emulating quantum teleportation of a Majorana zero mode qubit, Phys. Rev. Lett. **126**, 090502 (2021).

[53] N. Harle, O. Shtanko, and R. Movassagh, Observing and braiding topological Majorana modes on programmable quantum simulators, Nat. Commun. **14**, 2286 (2023).

[54] M. J. Rancic, Exactly solving the Kitaev chain and generating Majorana zero modes out of noisy qubits, Sci. Rep. **12**, 19882 (2022).

[55] T. Dvir, G. Wang, N. van Loo, C.-X. Liu, G. P. Mazur, A. Bordin, S. L. D. ten Haaf, Ji.-Y. Wang, D. van Driel, F. Zatelli, X. Li, F. K. Malinowski, S. Gazibegovic, G. Badawy, E. P. A. M. Bakkers, M. Wimmer, and L. P. Kouwenhoven, Realization of a minimal Kitaev chain in coupled quantum dots, Nature (London) **614**, 445 (2023).

[56] E. Artin, Theorie der zöpfe, Abhandl. Hamburg **4**, 47 (1925); Theory of braids, Ann. Math. **48**, 101 (1947).

[57] C. P. Williams, *Explorations in Quantum Computing*, Texts in Computer Science, 2nd ed. (Springer, Berlin, 2011).

[58] D. Collins, N. Linden, and S. Popescu, Nonlocal content of quantum operations, Phys. Rev. A **64**, 032302 (2001).

[59] A. Sorensen and K. Molmer, Quantum computation with ions in thermal motion, Phys. Rev. Lett. **82**, 1971 (1999); K. Molmer and A. Sorensen, Multiparticle entanglement of hot trapped ions, *ibid.* **82**, 1835 (1999).

[60] A. D. Corcoles, E. Magesan, S. J. Srinivasan, A. W. Cross, M. Steffen, J. M. Gambetta, and J. M. Chow, Demonstration of a quantum error detection code using a square lattice of four superconducting qubits, Nat. Commun. **6**, 6979 (2015).

[61] A. Barenco, C. H. Bennett, R. Cleve, D. P. DiVincenzo, N. Margolus, P. Shor, T. Sleator, J. A. Smolin, and H. Weinfurter, Elementary gates for quantum computation, Phys. Rev. A **52**, 3457 (1995).

[62] X. Xiao, J. K. Freericks, and A. F. Kemper, Determining quantum phase diagrams of topological Kitaev-inspired models on NISQ quantum hardware, Quantum **5**, 553 (2021).

[63] T. A. Bespalova and O. Kyriienko, Quantum simulationand ground state preparation for the honeycomb Kitaev model, arXiv:2109.13883.

[64] R. Schmied, J. H. Wesenberg, and D. Leibfried, Quantum simulation of the hexagonal Kitaev model with trapped ions, New J. Phys. **13**, 115011 (2011).

[65] L.-M. Duan, E. Demler, and M. D. Lukin, Controlling spin exchange interactions of ultracold atoms in optical lattices, Phys. Rev. Lett. **91**, 090402 (2003).

[66] B.-Y. Sun, N. Goldman, M. Aidelsburger, and M. Bukov, Engineering and probing non-Abelian chiral spin liquids using periodically driven ultracold atoms, PRX Quantum **4**, 020329 (2023).

[67] T. Cookmeyer and S. D. Sarma, Engineering the Kitaev spin liquid in a quantum dot system, Phys. Rev. Lett. **132**, 186501 (2024).

[68] H.-D. Chen and J. Hu, Exact mapping between classical and topological orders in two-dimensional spin systems, Phys. Rev. B **76**, 193101 (2007).

[69] X.-Y. Feng, G.-M. Zhang, and T. Xiang, Topological characterization of quantum phase transitions in a spin-1/2 model, Phys. Rev. Lett. **98**, 087204 (2007).

[70] H.-D. Chen and Z. Nussinov, Exact results of the Kitaev model on a hexagonal lattice: Spin states, string and brane correlators, and anyonic excitations, J. Phys. A: Math. Theor. **41**, 075001 (2008).

[71] J. Nasu, M. Udagawa, and Y. Motome, Vaporization of Kitaev spin liquids, Phys. Rev. Lett. **113**, 197205 (2014).

[72] J. Nasu, M. Udagawa, and Y. Motome, Thermal fractionalization of quantum spins in a Kitaev model: Temperature-linear specific heat and coherent transport of Majorana fermions, Phys. Rev. B **92**, 115122 (2015).

[73] K. L. Hur, A. Soret, and F. Yang, Majorana spin liquids, topology, and superconductivity in ladders, Phys. Rev. B **96**, 205109 (2017).

[74] M. Ezawa, Braiding and fusion of Majorana fermions in minimal Kitaev spin liquid on a single hexagon with 5 qubits, arXiv:2401.01051.

[75] T. Menke, W. P. Banner, T. R. Bergamaschi, A. Di Paolo, A. Vepsäläinen, S. J. Weber, R. Winik, A. Melville, B. M. Niedzielski, D. Rosenberg, K. Serniak, M. E. Schwartz, J. L. Yoder, A. Aspuru-Guzik, S. Gustavsson, J. A. Grover, C. F. Hirjibehedin, A. J. Kerman, and W. D. Oliver, Demonstration of tunable three-body interactions between superconducting qubits, Phys. Rev. Lett. **129**, 220501 (2022).

[76] S. P. Pedersen, K. S. Christensen, and N. T. Zinner, Native three-body interaction in superconducting circuits, Phys. Rev. Res. **1**, 033123 (2019).

[77] T. R. Bergamaschi, T. Menke, W. P. Banner, A. Di Paolo, S. J. Weber, C. F. Hirjibehedin, A. J. Kerman, and W. D. Oliver, Distinguishing multispin interactions from lower-order effects, Phys. Rev. Appl. **18**, 044018 (2022).

[78] Ye.-M. Zhan, Yu.-Ge. Chen, B. Chen, Z. Wang, Y. Yu, and Xi. Luo, Universal topological quantum computation with strongly correlated Majorana edge modes, New J. Phys. **24**, 043009 (2022).

[79] J. Franko, E. C. Rowell, and Z. Wang, Extraspecial 2-groups and images of braid group representations, J. Knot Theory Ramif. **15**, 413 (2006).